UCRL-100259
PREPRINT

MOLECULAR DYNAMICS AND IRREVERSIBILITY, FROM BOLTZMANN TO NOSÉ

William G. Hoover
Department of Applied Science
University of California at Davis
and
Department of Physics
Lawrence Livermore National Laboratory
University of California
Livermore, CA 94550

This paper was prepared to be presented at
The Boltzmann Seminar
Hohe Wand, Austria
January 1989

January 1989

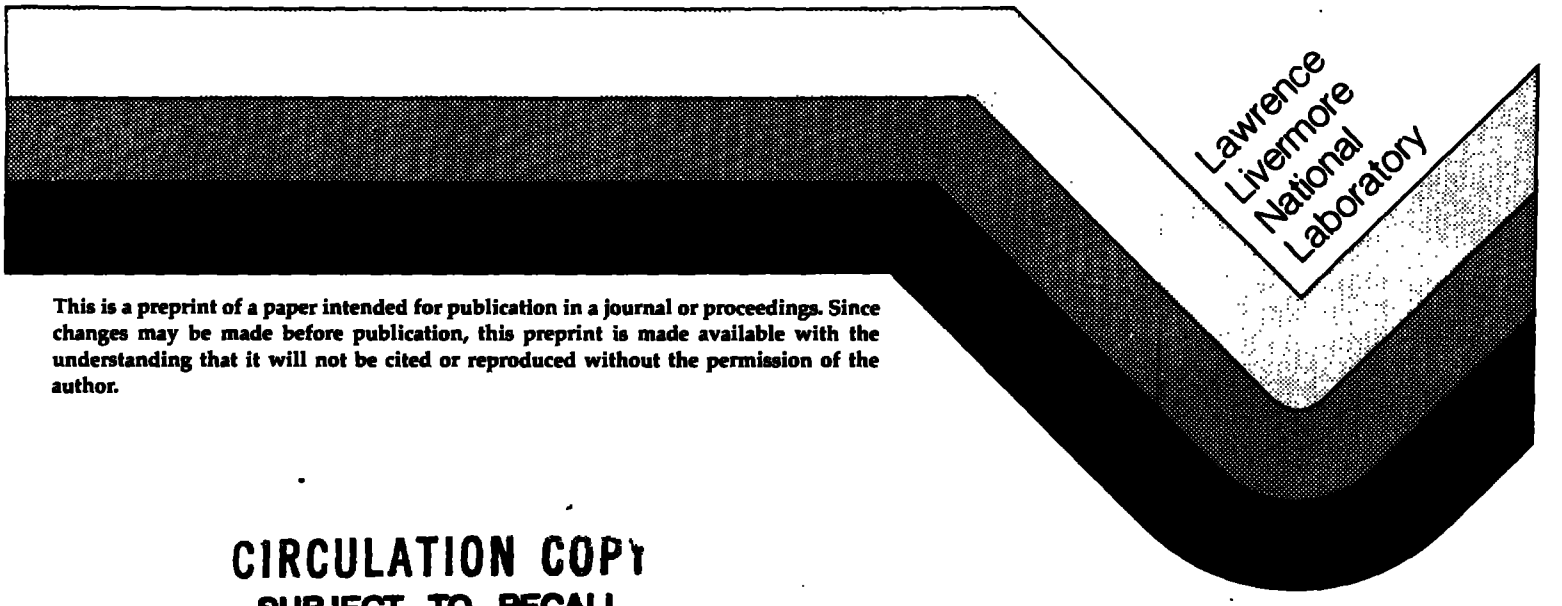

Molecular Dynamics and Irreversibility, from Boltzmann to Nosé*

William G. Hoover

Department of Applied Science
University of California at Davis and
Department of Physics
Lawrence Livermore National Laboratory
Livermore, California 94550 USA

* This work was performed under the auspices of the United States Department of Energy under University of California-Lawrence Livermore National Laboratory Contract Number W-7405-Eng-48.

Abstract:

Throughout Boltzmann's life-long atomistic study of irreversibility, he emphasized the one-body distribution function f_1, averaged over many particles, with the underlying dynamics taken to be a series of two-body collisions. His derivation of the H Theorem, linking dynamics and thermodynamics, remains *the* major accomplishment in understanding the Second Law of Thermodynamics. Today his analytic one-body approach has largely been superceded by using fast computers to simulate many-body "Molecular Dynamics".

Fermi originated Molecular Dynamics at Los Alamos in 1953. His few-body one-dimensional chains launched a generation of numerical studies of Lyapunov-unstable ordinary differential equations. By 1972 computers could simulate 1000-body gases, liquids, or solids, and a new nonequilibrium mechanics was developing to facilitate this work. In 1984, Nosé made a major contribution. He showed how to introduce macroscopic variables, such as temperature, pressure, and heat flux, directly into time-reversible microscopic equations of motion.

When Nosé's mechanics is applied to nonequilibrium systems zero-volume "strange attractors" form in the many-body phase space. The attractors provide a new explanation for the classical problem of irreversibility that fascinated Boltzmann. Here I trace the evolution of molecular dynamics from Fermi's work at Los Alamos to Nosé's recent work, and I speculate on the applicability of the new nonequilibrium ideas to quantum systems.

Table of Contents

1. Boltzmann, the H Theorem, and Molecular Dynamics

It is fast computers that make molecular dynamics possible. The resulting dynamical simulations link the time-*reversible* fundamental viewpoint of microscopic mechanics to Boltzmann's microscopic, but approximate, kinetic theory, as well as to the phenomenological and time-*irreversible* macroscopic viewpoints of thermodynamics and hydrodynamics. These computer links among fundamentals, theory, and phenomenology change not just our point of view, but also our knowledge and our way of thinking about physics. In this review I describe these changes, beginning with Fermi's seminal calculations at Los Alamos, and ending on the presentday research frontier.

Both the underlying conceptual basis and the mathematical methods of molecular dynamics predate Boltzmann. Even today, the mechanical equations of Newton, Hamilton, and Gauss are solved with ancient algorithms based on Taylor's expansion. But before computers an algorithmic attack on molecular dynamics was premature. Maxwell and Boltzmann built kinetic theory from classical mechanics by averaging over space and time[1,2] in order to avoid a head-on attack on the many-body problem.

The most significant technical difference between today's computer calculations and Boltzmann's hand calculations is raw speed. This difference in speed is responsible for differences in attitude and in goals. Boltzmann didn't think seriously about calculating *all* the trajectories in a many-body system. It was impossibly complicated. As an alternative, Boltzmann

introduced distribution functions in order to average over calculations too time-consuming to contemplate.

The situation is very different today. Historic textbook complaints bemoaning our inability to solve the equations of motion are obsolete. Right now the computers are about twelve orders of magnitude faster than humans. And parallel processing promises to increase the ratio much more. Now computers make it simpler to solve the original trajectory problem than to work out the average distribution functions. The trajectories are generated in discrete steps. The complicated molecular trajectories are divided up into simpler "timestep" sections, each of which can be worked out analytically. Linking these timesteps together generates an accurate trajectory. To illustrate, Figure 1 displays an approximate harmonic-oscillator trajectory[3]. The exact trajectory is an ellipse. The approximation used in the Figure is typical for numerical work. It is the fourth-order Runge-Kutta algorithm. With the normal timestep choice, one-sixtieth of the oscillator period, the error in the Runge-Kutta approximation is much too small to see. In the Figure I use *six* steps per period rather than sixty, thereby increasing the energy error by a factor of one hundred thousand and making it possible to see two different errors associated with the numerical method. First, the *amplitude* gradually decreases. Second, the *phase* is shifted. Both errors are negligibly small for reasonable timestep choices.

The approximate oscillator trajectory shown in the Figure captures the style of the approximate trajectories used in molecular dynamics studies. By the term "molecular dynamics" we simply mean such a numerical

solution of the classical equations of motion, usually for many bodies. Given the forces, the only approximation is the use of a finite time step. Normally the effect of that approximation is demonstrably negligible relative to statistical errors. The many-body molecular dynamics trajectories can then replace, if they cover phase space well enough, the idealized continuous one-body distributions introduced and studied by Maxwell and Boltzmann. This reversal, from one-body distributions to many-body trajectories, occurred only because ordinary differential equations are more easily solved numerically than are partial differential equations.

The origins of kinetic theory were European. In 1905 Mrs. Hearst persuaded Boltzmann to leave the pleasant sophistication of Vienna for a summer in California. His account of that summer is delightful reading [4]. He lectured at Berkeley on irreversible processes, his favorite research topic. He visited Livermore, Monterey, and the new Lick telescope at Mount Hamilton. While surviving the stress of California's rough roads, local prohibition, and western cuisine, Boltzmann clearly saw the future, expecially in the potential of Mrs. Hearst's University of California.

A generation later, the United States set the pace in computation, and did so for another generation, using World War II's scientific immigrants to develop and implement differential equations on the world's most powerful computers. While the war was on, these were handcranked machines. But the bombs that ended the war demanded ever more complex calculations. By 1952 the Los Alamos "MANIAC" computer was about a million times faster than humans[5]. That amazing speed has now increased by another factor of a million. And the once-rural institution at which Boltzmann lectured, the University of California, now controls more CRAYS and more scientific computing power than any other institution in the world.

II. Molecular Dynamics Begins at Los Alamos and Livermore.

Continually-growing computer power fosters ever more complex physics problems. And there is no limit to this growth. The most-interesting physics is nonlinear and "chaotic". In a chaotic problem small changes in initial conditions lead to big differences in the solutions[6-8]. Turbulence is such a problem. These problems are infinitely harder to solve by hand than are linear ones. But nonlinearity is no problem for computers. They give us a highly-accurate approximate solution.

At Los Alamos, computers were vital to predicting and understanding short-time highly-nonequilibrium bomb experiments. Patriotism attracted many of the world's most talented and stimulating scientists to this work. They speculated on the applicability of growing computer power to other areas in mathematical physics. Computation moved from hand calculators to punched cards in 1943, under Feynman's supervision. The war ended and nearly ten years passed before Los Alamos' stored-program MANIAC computer was ready.

Fermi moved to Chicago after the war. He remarked that he would have stayed at Los Alamos had it been a University. But Fermi still returned in the summers, to work with Metropolis, Teller, Ulam, and other pioneers. Fermi had invented one useful many-body technique, the Monte-Carlo method, long before his Los Alamos days. The dynamic many-body problem, hard even for three bodies, remained a natural challenge in mechanics. After the war, as a summer commuter from Chicago, he

introduced a primitive molecular dynamics at Los Alamos.

Fermi wanted to link molecular dynamics and thermodynamics, by watching the Second Law of Thermodynamics in action. To do this he simulated the motion of many-body chains of the type displayed in Figure 2. His idea was to watch many-body systems approach equilibrium [9], and to compare the results to the predictions following Boltzmann's one-body H-theorem route. Though short computer runs worked fine, one day an overlong computation seemed to reverse and back away from equilibrium. There was no error. The backup was real. For studying the approach to equilibrium, Fermi's choice of system was unfortunate. He did not realize that one-dimensional chains do not equilibrate nearly as easily as do two- and three-dimensional systems. The failure of the chains to equilibrate surprised Fermi and helped awaken widespread interest in deterministic chaos in the next two decades.

Teller wanted a laboratory to compete with Los Alamos. The new rival, the Lawrence Radiation Laboratory, at Livermore, took shape while Los Alamos' MANIAC computer was being developed. At Livermore, Alder and Wainwright soon tested Boltzmann's one-body H-Theorem analysis of the approach to equilibrium[10]. They studied the motion of 100 three-dimensional hard spheres. These many-body hard-sphere studies confirmed Boltzmann's equilibration analysis. Alder and Wainwright's further studies were conclusive in showing that the freezing transition, and the existence of the solid phase, depends only on repulsive forces. The time-exposure trajectories shown in Figure 3 document

this early work[11]. Also significant was the quantitative agreement of the molecular dynamics calculations with Wood and Parker's Monte-Carlo simulations of the same systems. The two numerical techniques were found to agree not just in the thermodynamic limit, but even for systems of just a few particles[12].

These early demonstrations that thermodynamic phase equilibria, as well as the approach to equilibrium, could be modelled with just a few interacting particles, established the utility of molecular dynamics in linking microscopic and macroscopic behavior. At last Maxwell and Boltzmann's conceptual basis linking fundamental microscopic approaches, molecular dynamics, kinetic theory and statistical mechanics, to phenomenological macroscopic approaches, thermodynamics and hydrodynamics, was secure. There was no longer any real doubt that microscopic many-body dynamics could reproduce macroscopic behavior. It was simply a question of figuring out how to do it as quickly, easily, and efficiently as possible.

III. Applications to Real Solids and Liquids at Brookhaven, Argonne, and Orsay.

Across the country from Alder and Wainwright's California calculations with idealized hard spheres, Vineyard, at Brookhaven on Long Island, simulated the behavior of real irradiated copper crystals. Vineyard demonstrated the applicability of the many-body molecular-dynamics techniques to real atomic-scale problems involving the interaction of high-energy radiation with matter. His results appeared first on the cover of the Journal of Applied Physics, reproduced here as Figure 4.

The conception, execution, and description of these early calculations were models of simplicity and clarity. Vineyard characterized nonequilibrium energy storage following high-energy irradiation. He studied radiation damage by scattering energetic particles from crystals, following the individual collisions, with the viscoelastic boundaries draining off heat to reduce the effect of small system size. He established the importance of "focussing collisions", which transmit energy, coherently and through long distances[13].

Long before these early days of molecular dynamics, equilibrium gases and solids were fairly well understood. Gases could be treated as nearly-independent particles, while solids could be treated as nearly-independent phonons. Liquids were more mysterious. In principle, the known many-body equilibrium distribution function could be integrated over N-2 particle coordinates, to find the two-body distribution function needed to understand pressure and energy. But this averaging was too involved

for practical calculations. A generation of physicists developed complicated distribution-function theories to discuss liquids[14], but little actually emerged before computer simulation. With fast computers this generation's theory became obsolete. After a period of testing, the old approaches, integral equations, cell models, and virial series, could be retired, replaced by perturbation theory.

In the early days of molecular dynamics, "solving" another many-body problem had meant making another computer simulation. But by 1970, perturbation theory[15] made possible quantitative predictions of many-body thermodynamic properties in terms of *reference* computer data. The basic two-body "reference-system" properties were taken from computer experiments. A crude example is shown in Figure 5, where the Lennard-Jones-pair-potential and argon phase diagrams are displayed together. The Lennard-Jones potential is not a specially faithful representation of argon, but is certainly a reasonable reference-system basis for perturbation calculations. And the perturbation theory worked well for "simple liquids", meaning monatomic fluids like argon.

With reference-system properties for hard spheres established at Los Alamos and at Livermore, the idea of describing liquids, using the more-realistic continuous-potential case, was acted on by Rahman. Rahman, working alone at the Argonne Laboratory near Chicago, took on an outstanding hard-but-tractable problem in equilibrium statistical mechanics, the modelling of an equilibrium monatomic liquid. Rahman[16] was the first to study a realistic liquid with molecular dynamics and to compare the results with experimental data. The

structures that he found with 864 atoms were in agreement with laboratory experiments and inspired further molecular-dynamics studies of equilibrium liquids.

Rahman also measured the equilibrium time-correlation functions needed to generate the linear transport coefficients. Soon after, Verlet, Levesque, and Kürkijarvi, in France, took up molecular dynamics and carried out definitive studies of both thermodynamic and transport properties of the prototypical Lennard-Jones liquid[17]. Since then, with spreading computer power and interest, molecular dynamics has become a truly international enterprise[18]. To illustrate this idea, but without any attempt at completeness, I mention as examples Evans in Australia, Posch in Austria, Bellemans in Belgium, Klein in Canada, Singer in England, Hansen in France, Hess in Germany, Berendsen in Holland, Rapaport in Israel, Iacucci in Italy, Nosé in Japan, Barojas in Mexico, Dremin in Russia, and Toxvaerd in Sweden.

Most liquids are polyatomic, not monatomic and "simple", and the classical treatment of polyatomic molecules has remained a subject of theoretical speculation. Many successful numerical simulations have appeared[18,19]. The viscosity for butane, for instance, has been investigated by two completely independent methods[20] and both simulated results lie within about 25% of the experimental viscosity. The simulation of large biological molecules followed naturally[21], as did also solid-phase applications in materials science[22], but with remaining major uncertainties with respect to the forces and the effect of quantum mechanics on the dynamics. The main motivation for undertaking large-molecule studies is the rapidly-improving resolution of experimental techniques. See Figure 6 for a recent detailed scanning-tunneling-microscope snapshot of DNA[23].

IIII. Molecular Dynamics Far From Equilibrium.

Equilibrium Newtonian molecular dynamics was expected to give accurate transport coefficients--diffusion, viscosity, and thermal conductivity--through Green and Kubo's fluctuation theory, but the agreement with experiment turned out to be poor. The early many-body simulations of liquid transport properties contained errors. The calculated triple-point viscosity of liquid argon, assuming a pairwise-additive Lennard-Jones potential for the interatomic forces, was considerably too high. The thermal conductivity was worse, different from experiment by a factor of two, much too much to explain on the basis of force-law uncertainty. Thus, resolving disagreements between the equilibrium fluctuation theory[17] and experiment was one of the main motivations for the early nonequilibrium simulations[24]. Ashurst set out to measure liquid transport properties by a direct nonequilibrium method, simulating laboratory flows with what he called "Nonequilibrium Molecular Dynamics". Independent related work, but on a smaller scale, was then being carried in England by Gosling, McDonald, and Singer[25], and by Lees and Edwards[26].

Transport properties are mainly of interest not for checking fluctuation theory, but for use in hydrodynamic simulations of nonequilibrium flows. Of course sufficiently simple flows can be used to find the transport coefficients themselves. Nonlinear simulations of *driven* systems, in nonequilibrium steady states were studied at length by Ashurst in his Ph. D. thesis work at Livermore[24]. He developed time-reversible momentum and heat reservoirs which could be used to drive shear

flows and heat flows while maintaining steady boundary temperatures. The boundaries he used, after trying out many less-satisfactory alternatives, are shown in Figure 7.

Ashurst had no vested interest in the use of the tradiational classic time-irreversible Langevin and Fokker-Planck stochastic equations. Instead, his instincts led toward time-reversible methods. The time-reversal-invariance of his nonequilibrium equations of motion is essential to the understanding of irreversibility discussed in Section VI. His boundary-driven work led to the steady-state generalization of homogeneous-deformation dynamics developed independently by Lees and Edwards[26]. Ashurst devoted serious attention to boundary conditions, exploring a variety of rigid and periodic boundaries, both fixed and in motion. This work led directly to shear and bulk deformation methods used to study viscosity and plasticity, identical to those formalized independently by Andersen[27] and Parrinello and Rahman[28] to describe the equilibrium constant-pressure and constant-stress ensembles.

To offset thermal fluctuations, molecular dynamics was typically applied to highly-nonequilibrium problems. These were indeed *very* far from equilibrium, although not *so* far away as conditions in a strong shockwave. In the dynamical shockwave simulations temperature changed by thousands of degrees, and pressure by half a million atmosopheres, in a shockwidth of a few atomic diameters. The nonequilibrium simulations showed, in qualitative agreement with experiment, a small but definite decrease in viscosity with strain rate. The change of conductivity with increasing temperature

gradient could be either an increase or a decrease, depending on the temperature.

With non-Newtonian boundary conditions a variety of new simulation types became possible. Nonequilibrium simulations could include moving periodic boundaries. Volume and shape changes could be imposed homogeneously or through displacements induced by fields or localized at physical boundaries. These possibilities are illustrated in **Figure 8**. The first calculations confirmed that the various approaches gave consistent results[24]. At Los Alamos, strong shockwaves[29] were simulated by contracting boundaries. The results were not very different from the linear-transport Navier-Stokes predictions, despite gradients much larger than those typically used in nonequilibrium simulations. Thus the nonlinear behavior of the transport coefficients in shockwaves is very different from that found in the gentler homogeneous deformations. Despite the very large gradients shockwave transport coefficients are close to the zero-gradient linear-transport values. This insensitivity to nonlinearity is still largely unexplained, though some fundamental low-density kinetic-theory studies have been carried out[30]. Years later the reversed case, expansion, was used to study fragmentation[31,32] and fracture[33], as shown in **Figures 9 and 10.**

Eckart Meiburg, in Gœttingen, was the first to carry out large-scale hydrodynamic simulations with molecular dynamics[34]. Besides the shockwave work, earlier less-extensive smaller-scale studies[35,36] had likewise suggested that molecular dynamics and hydrodynamics match closely. Computers were becoming powerful enough to consider again averaging to measure

distribution functions. A typical averaged flow field taken from Meiburg's Master's-thesis work is shown in Figure 11. In that Figure each of Meiburg's arrows stands for the velocity averaged over about fifty separate atoms. Like Vineyard's, his work is a model of clarity. He studied the motion of tens of thousands of hard spheres flowing past an obstruction and observed an average flow field looking very much like the initiation of a von-Karman vortex street.

More recently, Mareschal, Kestemont, Mansour, and Puhl[37] have studied Rayleigh-Bénard instability, in which a fluid heated from below, in a gravitational field, develops cylindrical convection currents. A typical averaged flow field distribution in shown in Figure 12. They made a careful comparison of molecular-dynamics results with hydrodynamic solutions of the Navier-Stokes equations. The Rayleigh-Bénard model is of special historic interest through its link to the computational study of chaos introduced in Lorenz'[38] classic paper on atmospheric turbulence which appeared in 1963.

V. Irreversibility and Instability from Time-Reversible Two-Body Mechanics

Both Newton's and Schrœdinger's equations of motion are "time-reversible". This means that any movie illustrating a Newton or Schrœdinger solution can be run either backward or forward through the movie projector. Both versions satisfy the same equations of motion. In the reversed direction, the Newtonian velocities would change sign, as would the corresponding imaginary component of Schrœdinger's wave function, but the time-reversed classical trajectory, or quantum probability density, is as good a solution of the equations of motion as the forward one.

The conflict between these fundamental time-reversible descriptions of motion and the even-more-fundamental irreversible behavior of the "real" world has attracted continuing interest since Boltzmann's time. Boltzmann focussed attention on the time evolution of the averaged one-body probability density, $f_1(q,p,t)$.

The gas-phase Boltzmann equation for the time-development of f_1, as well as the linearized Krook-Boltzmann approximation, and the Fokker-Planck plasma equation, all evolved from analytic attempts to express and understand patently-irreversible many-body phenomena in terms of the one-body distribution function. These simplifications are less necessary today. We can follow the details of phase-space deformation, as given by the the time history of the N-body distribution function f_N, for 32-body systems. Today we can generate accurate trajectories for a million particles. And particle mechanics has itself been modified to treat the problems addressed by Boltzmann, Fokker, and Planck. A 1984

modification of Hamiltonian mechanics, discovered by Shuichi Nosé and described in Section VI, is the key to these modern trajectory investigations of irreversible behavior.

Boltzmann studied the one-particle distribution function in dilute nonequilibrium gases. His time-*irreversible* Boltzmann equation

$$df1/dt = (\partial f1/\partial t)_{collisions} ,$$

provided a plausible description averaged over a large number of particles. By ignoring fluctuations and correlations, Boltzmann estimated the time-dependence of the one-body-phase-space probability density. His most famous result, derived from the Boltzmann equation, was the H Theorem. That theorem shows that isolated systems irreversibly approach equilibrium. Thus, Boltzmann's equation already lacked the time-reversibility of Newtonian mechanics and provided an approximate entropy function which could not decrease with time.

The fundamental mechanism underlying the approach to equilibrium is now known to be "Lyapunov instability"[39-43]. This instability, and its many-body generalization to the "Lyapunov spectrum", describes the exponential spreading apart of initially-neighboring many-body-phase-space trajectories, as well as the exponential growth, or decay, of many-dimensional phase-space hypervolumes. See Figure 13. The trajectory spreading has to be simultaneously accompanied by an orthogonal compression because *any* Hamiltonian flow, when averaged over all directions in the phase space, is incompressible. The orthogonal rates

of growth and decay of phase-space separation are given by "Smale Pairs" of Lyapunov exponents, equal in magnitude but opposite in sign. The idea of measuring distance between points in phase space might seem bizarre, because coordinates, momenta, and friction coefficients all have different physical units. But because the growth and decay rates are *exponential*, the muliplicative choice of scales of the axes are irrelevant. Exactly the same exponents would result for any other choice of generalized coordinates and momenta.

In phase space, the spreading instability progresses from small scales, with hyperspheres elongating into hyperellipsoids, to large scales, at which the deforming hyperellipsoids must bend to follow the macroscopic phase-space motion. On the infinitesimal microscale the Lyapunov instability can be seen as sensitive dependence on initial conditions, as revealed by a linear stability analysis of the equations of motion.

Figure 14 shows a simple example, the Newtonian Lyapunov-unstable bouncing of two balls in a constant vertical gravitational field. The lower of the balls is held fixed. For clarity, the upper, moving ball is shown as a mass point. In cartesian laboratory coordinates the bounces become more widely separated with each bounce. In semilogarithmic coordinates the exponential instability of the motion is clearly apparent.

In many-body phase space the generalized exponential Lyapunov instability is described by the Lyapunov spectrum[41-43]. **Figure 15** shows typical many-body spectra for both two- and three-dimensional fluids and solids. The Smale-pair symmetry of these equilibrium spectra follows from the equivalence of

forward and backward solutions of the equations of motion. In nonequilibrium steady states, this symmetry is broken, and the sum of the Lyapunov exponents is negative.

VI. Irreversibility from Time-Reversible Many-Body Mechanics-Nosé's Modification of Hamiltonian Mechanics

Molecular dynamics replaced a generation of cumbersome, inadequate, approximate one-body and two-body theories with simple, accurate many-body computer experiments. But appropriate analyses of these experiments required new ideas suited to computation. This had to wait for a new generation of scientists brought up to use the computer as a tool, for which new techniques could be specially designed.

An advance was made by setting aside the irreversible stochastic approximations well-suited to slower hand calculations, but not so well-suited to understanding deterministic trajectory development far from equilibrium. The classical Langevin and Fokker-Planck equations had previously been used to impose temperature, but these approaches are time-irreversible. The simplest derivation of the Fokker-Planck equation[44], for instance, assumes an acceleration proportional to the momentum gradient of a local entropy:

$$\Delta(dp/dt) \propto \nabla_p \{\ln[f(p)/f_{equilibrium}(p)]\}.$$

Reversing the sign of the time leaves the left side unchanged while changing the sign of the right side, revealing the time-*irreversible* approximate character of the Fokker-Planck equation.

Nosé, from Japan, but working in Canada with Mike Klein, made the necessary conceptual breakthrough. Nosé[45] discovered a reversible deterministic form of Hamiltonian mechanics which reproduces the thermal canonical distribution. His temperature-dependent reversible equations describe something like a microwave oven, but capable of cooling reversibly as well as heating. The Hamiltonian basis of his work is important for two different reasons. First, the equations of motion, either at or away from equilibrium, are time-reversible, making possible an exact analysis of thermodynamically-irreversible processes. Second, the Hamiltonian basis suggests extensions of Nosé's classical ideas to quantum dynamics and quantum statistical mechanics. Despite these two advantages, his original derivation was unnecessarily complex. But the result is simple, a set of many-body equations of motion, containing the equilibrium temperature T and at least one friction coefficient ζ:

$$dp/dt = F(q) - \zeta p \quad ,$$

where the friction coefficient ζ, rather than being constant, is itself determined by a temperature-dependent time-reversible integral feedback equation:

$$d\zeta/dt = \Sigma[(p^2/mkT) - 1]/\tau^2 \quad ,$$

with an arbitrary relaxation time τ. Thus the friction coefficient ζ increases in those parts of phase space with above-average temperature and decreases in those parts where the temperature is below average.

Nosé's derivation of his equilibrium equations of motion was relatively complicated. A simpler way to derive these same equations of motion is to ask the question Brad Holian posed: "What friction coefficient ζ generates the canonical distribution[46]?" A whole series of "Nosé-Hoover" equations of motion, based on the various velocity moments $\langle p^{2n} \rangle$ can similarly be derived[47].

At equilibrium, or in the nonequilibrium linear-response regime, Nosé's ideas simply reproduce Newtonian mechanics, with time-averaged macroscopic deviations of order 1/N for N-particle systems[48]. But Nosé's ideas can also be used to drive many-body systems away from equilibrium, with external forces, into thermostatted nonequilibrium steady states maintained by one or more Nosé thermostats[49]. Then concepts and methods borrowed from nonlinear dynamics can be used to determine and describe the structure of the resulting phase-space distributions. Once Nosé announced his discovery, Ashurst's work was recognized as a special case of Nosé's more-flexible feedback recipe.

At equilibrium Nosé discovered a new way to generate the equilibrium phase-space distribution f_N. In the more complex cases away from equilibrium, something more interesting happens. In any such case heat is exchanged. It can then be proved that *any* such nonequilibrium steady state *always* produces a *fractal* phase-space dimensionality, with an occupied phase-space dimension reduced below the equilibrium dimensionality[50-52]. The amazing result that these distributions *never* become continuous, no matter how fine the scale of observation, is, for the many-body

problem, as exciting and surprising a development as was the discovery of chaos in mechanics. And that discovery, which dates back to Poincaré, is viewed by many as revolutionary for physics today[6-8,53].

What are these ubiquitous fractal objects that characterize nonequilibrium systems? Fractal objects have been used in films to represent mountains, clouds, and water. A recent computer-generated magazine cover using fractals as a tool, is shown in Figure 16. A simpler fractal object is the Sierpinski sponge[54], shown in Figure 17. In any fractal the number of pairs of points varies in a regular way with distance. If one defines a dimensionality for such an object, by asking for the number of pairs of points lying within a radius r, that dimensionality is typically *not* an integer. For the sponge of Figure 17 the number of pairs of points within a small distance r of each other varies as $r^{2.727}$. Thus the sponge is said to have fractal dimensionality of 2.727. The object behaves like a fractional-dimensional "fractal" object. That these strange objects describe phase-space flows was probably unknown to Boltzmann. They are beautifully illustrated and described in Gleick's book on Chaos[6].

Developing and demonstrating these ideas required high-speed computer graphics. Even so, phase-space fractals are hard to display in the many-body case. About the simplest steady-state phase-space fractal distribution illustrates the one-body Galton-Board example[55] shown in Figure 18. In this example a single mass point falls through a periodic array of scatters. The accelerating "gravitational" field is downward, and the motion is made isokinetic, with the particle falling at constant speed, by applying Gauss'

Principle of Least Constraint [47,55]. The resulting phase space is only three-dimensional. In the Figure a phase-space cross section representing 10,000 successive collisions is shown. The distribution of distances between pairs of points in the cross section is consistent with a fractal dimensionality of about 1.5.

Figure 19 shows two separate ensembles, each with 2500 separate Galton Boards developing in time. Initially the ensemble members are distributed uniformly over two quadrants of the square phase-space cross section. The successive images show the ensemble members after 1, 2, 3, 5, and 10 collisions. Note that the ensembles' cross sections are approaching the single-trajectory Poincaré section shown in Figure 18. Similar calculations have been carried out for a low-density shear-flow analog of the Galton Board, using both molecular dynamics[56] and the Boltzmann Equation[57].

Nosé's idea, generalized to nonequilibrium systems, made possible the marvelous marriage of three parties, mechanics, nonlinear dynamics, and irreversible thermodynamics[50-52]. The new mechanics, with Nosé's computational thermostats built in, showed that nonequilibrium phase-space distributions are *typically* fractal, just like the one-body Galton Board problem illustrated above. The necessary geometric concepts are not so new. The basic idea of phase-space mixing was known to Poincaré and the mathematics of strange sets had been around for about fifty years when Nosé pointed the way toward a new synthesis.

With Nosé's dynamics the phase-space deformation of nonlinear dynamics, the heat reservoirs of nonequilibrium molecular dynamics, and the inexorable

entropy increase of irreversible thermodynamics could all be linked together. The logical connections among these three concepts involve the three steps indicated in Figure 20:

I. Conservation of comoving probability in mechanical phase-space flows, relating the time-rate-of-change of the many-body distribution function to the corresponding time-rate-of change of phase volume.

II. Steady time-development of phase-volume from nonlinear dynamics, relating the sum of the Lyapunov exponents to the sum of Nosé's friction coefficients through Nosé's equations of motion.

III. Linking the diminishing phase-space volume with thermodynamics through the heat reservoirs implicit in Nosé's equations of motion. This last step establishes that the impossibility of phase-space growth, in the steady state, is equivalent to the macroscopic Second Law of Thermodynamics.

To begin with step I, *any* mechanical flow in phase space satisfies a "continuity equation", with conservation of the total number of systems studied. To illustrate, consider the continuity equation of fluid mechanics,

$$\partial\rho/\partial t + \partial(\rho u)/\partial x = 0 \ ,$$

where ρ is the mass density and u is the stream velocity. The typical textbook derivation of the continuity equation proceeds by setting the change in mass in a fixed "Eulerian" volume element $dxdydz$ equal to the flow

through the boundaries. This flow is proportional to the flux ρu. The only additional assumptions required to derive the continuity equation are (i) the differentiability of the flow velocity and density and (ii) the lack of sources or sinks. From the continuity equation the *comoving* density derivative (that is, the "Lagrangian" derivative following the motion) can be computed:

$$d\rho/dt = \partial\rho/\partial t + u\,(\partial\rho/\partial x) = -\rho(\partial u/\partial x)\ ,$$

Dividing by the density gives a more elegant logarithmic form:

$$d\ln\rho/dt = -(\partial u/\partial x)\ .$$

The divergence of the velocity, $\partial u/\partial x$, the sum of the orthogonal strain rates, is also the logarithmic rate of volume change:

$$(\partial u/\partial x) = d\ln V/dt\ .$$

Thus the continuity equation for fluid flow takes the form:

$$d\ln\rho/dt = -d\ln V/dt\ .$$

or

$$d\ln\rho/dt + d\ln V/dt = 0.$$

Exactly the same idea can be applied to the flow of many-body probability fluid in the many-body phase space. In that case the density function ρ is replaced by the N-body probability density f_N and the volume V is

replaced by the 6N-dimensional phase-space hypervolume $\otimes$. Then the corresponding "continuity" equation for the flow of phase-space probability can be written

$$d\ln f_N/dt + d\ln\otimes/dt = 0 , \qquad (1)$$

where $\otimes f_N$ is the total number of systems in the phase-space hypervolume $\otimes$.

In the second step 11 above, the Lyapunov exponents used in analyzing many-dimensional flows[43] are introduced in order to describe the time-averaged expansion and contraction of the phase-space volume $\otimes$. The exponents give the time-averaged rates of stretching and shrinking of the principle axes of a deforming hyperellipsoid in the phase space. In nonlinear chaotic systems the stretching and shrinking occur *exponentially* fast in time, varying as $\exp[\lambda t]$. See again **Figure 15.** The sum of these exponents $\{\lambda\}$ gives the rate at which phase-space volume changes:

$$d\ln\otimes/dt = \Sigma\lambda .$$

Nosé's equations of motion satisfy identically the relation

$$d\ln f_N/dt = \Sigma\zeta .$$

Combining these results with (1) above relates Nosé's friction coefficients to the Lyapunov exponents:

$$\Sigma\zeta = d\ln f_N/dt = -d\ln\otimes/dt = -\Sigma\lambda . \quad (11)$$

Nosé's equations of motion also show directly that the time-averaged friction coefficients $\langle\{\zeta\}\rangle$ and the corresponding instantaneous temperatures $\langle\{p^2/mk\}\rangle$ are uncorrelated:

$$\Sigma\langle\zeta p^2/mk\rangle = \Sigma\langle\zeta\rangle\langle p^2/mk\rangle \ .$$

Thus, the lefthand side, the summed rates of heat extraction of the Nosé thermostats divided by the corresponding temperatures, $\{\langle p^2/mk\rangle\}$, is exactly equal to the sum of the Nosé friction coefficients. The last step III, then links dynamics to the Second Law of Thermodynamics through the friction coefficients $\{\zeta\}$ in Nosé's equations of motion:

$$-d\ln f_N/dt = -\Sigma\,\zeta = -(dS/dt)/k \quad , \ (III)$$

where the sum is over all such friction coefficients. The observation that the steady logarithmic rate of volume change, $d\ln\otimes/dt$, cannot be positive, and must vanish at equilibrium, leads to the conclusion

$$0 > d\ln\otimes/dt$$

away from equilibrium. This continuous decrease of phase-space volume in the nonequilibrium steady state establishes that Gibbs' equilibrium N-body entropy definition, $S = -k\langle\ln f_N\rangle$, cannot be used in such nonequilibrium steady states because the corresponding nonequilibrium S would approach minus infinity.

The steadily-decreasing phase-space hypervolume implies the full chain of relations

$$(dS/dt)/k = \Sigma\zeta = +d\ln f_N/dt = -d\ln\otimes/dt = -\Sigma\lambda > 0.$$

The resulting conclusion--<u>THE TOTAL ENTROPY MUST INCREASE</u>--is made possible only through the simple structure of the Nosé equations of motion. This total entropy includes that of the heat reservoirs in which any Nosé system is embedded. The Gibbs' entropy *diverges* for any nonequilibrium steady state. To see this, notice particularly that the many-body probability density $f_N(q^N,p^N,\zeta,t)$ diverges[51]. The Second Law of Thermodynamics, from the standpoint of Nosé mechanics, becomes equivalent to the observation that a steady-state distribution function must occupy a Lyapunov-unstable *subspace* with reduced dimensionality, a zero-volume "strange attractor". For such nonequilibrium systems, the Second Law of Thermodynamics is not simply a high-probability statement, as with Gibbs' Paradox, but instead a probability-one statement. This follows from the fact that the nonequilibrium distributions are zero-volume fractal objects.

To see this consequence of the fractal many-body distributions in more detail, consider time reversibility and Loschmidt's Paradox. Because the many-body equations of motion are time-reversal-invariant it is certainly true that the phase space must also contain a reversed "repellor" region, just like the attractor but with reversed velocities, in which the Second Law is violated. Despite the undoubted existence of the repellor the Second Law *cannot* be violated by observable motions[50-52]. This is because the reversed "repellor" solution <u>repels</u> rather than <u>attracts</u> nearby trajectories, and thereby acts as a phase-space *source* rather than a *sink*. It is an

unstable phase-space object. Hence the reversed repellor trajectories, which would theoretically violate the Second Law of Thermodynamics, can never be observed using Nosé's mechanics.

Thus Nosé's mechanics sheds new light on, and extends, Boltzmann's treatment of irreversible processes. In this extension, the relevant distributions are many-body rather than one-body distributions. The underlying dynamics is the exact many-body dynamics rather than Boltzmann's approximate one-body dynamics. With Nosé's mechanics the statements that (1) entropy production is positive, that (2) heat flows from hot to cold, and that (3) transport coefficients are positive, all correspond to rigorous consequences of the equivalent geometric observation that phase-space hypervolumes cannot grow in nonequilibrium steady states.

Of course, Nosé's treatment of nonequilibrium boundaries is not the only possible treatment. But it is important to recognize that hydrodynamic flows can be generated and maintained by a variety of equally-valid boundary conditions. Those features that are common to a variety of boundaries will be shared by Nosé's choice. His is simply the most useful because it simplifies the corresponding theoretical analysis.

VII. Speculation: Quantum Irreversibility using "Gaussian" Time-Reversible Schrœdinger Mechanics.

Gauss formulated mechanics on the basis of a single principle, his "Principle of Least Constraint"[58]. Gauss' Principle states that *any* dynamical constraint should be implemented by using the least possible force:

$$\Sigma(F_c^2/2m) \text{ minimum, or } \Sigma(F_c dF_c/m) = 0 \quad .$$

The sum runs over all degrees of freedom in the constrained system.

It is interesting that this Principle, when used to implement isothermal conditions, by constraining the kinetic energy, produces exactly the same motion equations

$$dp/dt = F - \zeta p \ ,$$

as does Nosé's isothermal mechanics, but with a definite value for Nosé's relaxation time τ, zero.

The current interest in chaos has led to extensive speculation on "quantum chaos", that is the quantum behavior of systems with classically-chaotic Hamiltonians[53,59]. The Schrœdinger equation is not well suited to these studies so that a variety of efforts have been made to extend it to apply to nonequilibrium open systems[60-62].

First, the Schrœdinger Equation is linear, so that steady solutions can only oscillate in time. Second, it describes only thermally-isolated systems, while the

simplest interpretations of irreversibility in classical systems involve open systems in which work is converted to heat through the operation of Nosé thermostats.

We can take Gauss' least-constraint idea[58] over into quantum mechanics by restricting the solution of a *constrained Schrœdinger Equation*, which incorporates the least possible change in the quantum equation of motion

$$(\partial\psi/\partial t)_{\text{Gauss}} = (\partial\psi/\partial t)_{\text{Schrœdinger}} - \Sigma(\lambda_i \nabla C_i) \quad ,$$

where the $\{\lambda_i\}$ are Lagrange multipliers chosen to satisfy the constraints $\{C_i\}$.

To illustrate, consider the quantum version of the simple problem introduced in Figure 18, a mass point moving through a Galton Board under the influence of an external field[55]. Then the Gaussian constraints $\{C_i\}$ correspond to fixing the total mass, momentum, and energy in the Board. The Gaussian Lagrange multipliers $\{\lambda_i\}$ perform work and extract heat. The steady-state nonequilibrium Schrœdinger equation then describes a steady flow of probability current with fixed mass and energy. The generalized forces expressed by the Lagrange multipliers provide momentum at exactly the rate required to offset the scattering by the Board. The more-general fluctuating constraint technique introduced by Nosé could alternatively be used, controlling generalized Lagrange parameters with integral feedback and allowing the mass, momentum, and energy to fluctuate about prescribed mean values. Here we consider explicitly the special case in which these flow quantities are fixed.

It is convenient to solve the Galton Board problem on a hexagonal finite-difference grid. To use such a grid approach, the spatial derivatives are replaced by finite differences. Then the Gaussian equations of motion become a set of coupled nonlinear first-order ordinary differential equations. These equations can be solved using the same Runge-Kutta method that applies for classical problems. Sample solutions, on a 41x41 grid, both transient and time-averaged, are shown in Figures 21-23. We anticipate that solutions of such problems will lead not only to distributions approaching the fractal distributions found classically. They will also reveal the quantum analog of Lyapunov instability which underlies the Second Law of Thermodynamics and the irreversibility that Boltzmann found to be so fascinating.

VIII. Summary.

The averaging introduced by Maxwell and Boltzmann disappeared for a while, with fast computers, but eventually reappeared with a vengeance when both trajectories, described by ordinary differential equations, and distributions, described by partial differential equations, could be found for the same problems. The intercomparison of these two approaches, using ideas based in computation rather than in hand calculation, has led to exciting advances in physics.

The distribution-function analysis of Boltzmann could be tested by the trajectory calculations of Fermi, Alder and Wainwright, Vineyard, Rahman, and Verlet, and, for the first time, validated in cases where the force law was known. The molecular dynamics calculations superceded the interest in approximate one-body and two-body distribution functions and stimulated the advancement of two-body perturbation theory as a way for "understanding" many-body systems. At the same time the realism introduced by Vineyard broadened the audience and has helped make molecular dynamics a useful tool for understanding far-from-equilibrium processes in such diverse fields as catalysis, drug design, fluid dynamics, and materials science.

Nonequilibrium calculations have demonstrated both the power and the limits of linear transport theory and showed that the boundary conditions are crucial in simulating and describing far-from-equilibrium systems. Finally, Nosé's novel approach made it possible to link deterministic microscopic mechanics with phase-

space distributions and irreversible thermodynamics, in a way which Boltzmann would have enjoyed.

Where is atomistic computer simulation headed today? A major trend is toward parallel processing, to avoid the speed and capacity limits of a single processor. This approach promises rapid orders-of-magnitude increases in speed and capacity. Another direction in which improving capacity may lead is toward simulating far-from-equilibrium quantum systems. The new techniques may well simplify the treatment of quantum systems which show chaos. It is for this reason that I append Erwin Schrœdinger to the list of precomputer architects of molecular dynamics shown in Figure 24, Boltzmann, Gauss, Hamilton, Lyapunov, and Newton.

IX. Acknowledgment

Preliminary drafts of this paper were prepared for a meeting in Rome, commemorating Boltzmann, sponsored by the Italian and Austrian Physical Societies. The talk was given a week earlier, in Austria, at Hohe Wand, in January 1989. I sincerely thank G. Battimelli, M. De Maria, and M. G. Ianniello, organizers of the Italian Meeting for their kind invitation to speak in Rome, and Professors Grosse and Posch, of the University of Vienna, for making my alternate presentation possible in Austria. My participation was supported by the Austrian Physical Society as well as by the University of California at Davis and at Livermore and the Lawrence Livermore National Laboratory. The work reported here involved the joint efforts and hard work of many people. Of these, Brad Holian, Harald Posch, Bill Moran, Art Walstead, Mark Waid, and my wife, Carol, deserve special thanks.

REFERENCES:

[1]. S. G. Brush, **Kinetic Theory**, Vol. 1, "The Nature of Gases and of Heat"; Vol. 2, "Irreversible Processes"; and Vol. 3, "The Chapman-Enskog Solution of the Transport Equation for Moderately Dense Gases" (Pergamon, Oxford,1965, 1966, and 1972).

[2]. L. Boltzmann, **Lectures on Gas Theory**(University of California Press, Berkeley, 1961), translated into English by S. G. Brush.

[3]. G. D. Venneri and W. G. Hoover, J. Comp. Phys. 73, 468(1987).

[4]. L. Boltzmann, "Journey of a German Professor to El Dorado", from **Populære Schriften**, (Leipzig, J. A. Barth, 1905), translated into English by O. and G. Heinz, (Naval Postgraduate School, Monterey, California, 1971).

[5]. H. L. Anderson, Los Alamos Science, Fall Number (14) (Los Alamos National Laboratory, Los Alamos, New Mexico,1986).

[6]. J. Gleick, **Chaos, Making a New Science**(Viking, New York, 1987).

[7]. H. G. Schuster, **Deterministic Chaos** (Physik-Verlag, Weinheim, FRG, 1984).

[8]. H. Bai-Lin, **Chaos** (World Scientific, Singapore, 1984).

[9]. J. L. Tuck and M. T. Menzel, Advan. Math. 9, 399(1972).

[10]. B. J. Alder and T. E. Wainwright, in "**Transport Processes in Statistical Mechanics**", Proc. IUPAP Symposium, Brussels, 1956 (Interscience, New York,1958), p. 97.

[11]. B. J. Alder and T. E. Wainwright, Scientific American 201(4),113(October,1959).

[12]. W. G. Hoover and B. J. Alder, J. Chem. Phys. 46, 686(1967).

[13]. G. H. Vineyard, in **Interatomic Potentials and Simulation of Lattice Defects**, P. C. Gehlen, J. R. Beeler, and R. I. Jaffee, eds., (Plenum, New York, 1972).
[14]. J. O. Hirschfelder, C. F. Curtiss, and R. B. Bird, **Molecular Theory of Gases and Liquids**(Wiley, New York, 1954).
[15]. J. A. Barker and D. Henderson, J. Chem. Phys 47, 2856 and 4714(1967); G. A. Mansoori and F. B. Canfield, J. Chem. Phys. 51, 4958(1969); J. Rasaiah and Stell, Mol. Phys. 18, 249(1970); H. C. Andersen, J. D. Weeks, and D. Chandler, Phys. Rev. A 4, 1597(1971).
[16]. A. Rahman, Phys. Rev. 136, A405(1964).
[17]. D. Levesque, L. Verlet, and J. Kürkijarvi, Phys. Rev. A 7, 1690(1973).
[18]. Proceedings, Enrico Fermi School on "**Molecular Dynamics Simulation of Statistical-Mechanical Systems**" Varenna, 1985, G. Ciccotti and W. G. Hoover, eds. (North-Holland, Amsterdam, 1986).
[19]. G. Ciccotti, D. Frenkel, and I. R. McDonald, **Simulation of Liquids and Solid** (North-Holland, Amsterdam, 1986).
[20]. M. Ferrario and J.-P. Ryckaert, Mol. Phys. 54, 587(1985); G. Maréchal, J.-P. Ryckaert, and A. Bellemans, Mol. Phys. 61, 33(1987); R. Edberg, G. P. Morriss, and D. J. Evans, J. Chem. Phys. 86, 4555(1987); R. Edberg, D. J. Evans, and G. P. Morriss, J. Chem. Phys. 87, 5700(1987).
[21]. H. J. C. Berendsen and W. F. Van Gunsteren, in Proceedings, Enrico Fermi School on "**Molecular Dynamics Simulation of Statistical-Mechanical Systems**" Varenna, 1985, G. Ciccotti and W. G. Hoover, eds. (North-Holland, Amsterdam, 1986).
[22]. M. W. Ribarsky and U. Landman, Phys. Rev. B 38, 9522(1988).

[23]. This image of DNA, covering a square region, 340Å on a side, and showing a vertical variation of 90Å, was kindly furnished by Dr. Wigbert Siekhaus of the Lawrence Livermore National Laboratory. See T. P. Beebe, Jr., T. E. Wilson, D. F. Ogletree, J. E. Katz, R. Balhorn, M. B. Salmeron, and W. J. Siekhaus, Science (to appear, 20 January 1989).
[24]. W. T. Ashurst, **Dense Fluid Shear Viscosity and Thermal Conductivity via Non-Equilibrium Molecular Dynamics**, (Ph. D. Dissertation, University of California at Davis-Livermore, 1974); W. T. Ashurst and W. G. Hoover, Phys. Rev. Letts. 31, 206(1973); W. G. Hoover and W. G. Ashurst, Adv. in Theo. Chem. 1, 1(1975).
[25]. E. M. Gosling, I. R. McDonald, and K. Singer, Mol. Phys. 26, 1475(1973).
[26]. A. W. Lees and S. F. Edwards, J. Phys. C. 15, 1921(1972).
[27]. H. C. Andersen, J. Chem. Phys. 72, 2384(1980).
[28]. M. Parrinello and A. Rahman, J. Appl. Phys. 52, 7182(1981).
[29]. B. L. Holian, W. G. Hoover, B. Moran, and G. K. Straub, Phys. Rev. A 22, 2798(1980); B. L. Holian, Phys. Rev. A 37, 2562(1988).
[30]. W. Loose and S. Hess, Phys. Rev. A 37, 2099(1988).
[31]. J. A. Blink and W. G. Hoover, Phys. Rev. A, 32, 1027(1985).
[32]. B. L. Holian and D. Grady, Phys. Rev. Letts. 60, 1355(1988).
[33]. W. T. Ashurst and W. G. Hoover, Phys. Rev. B. 14, 1465(1976); B. Moran, **Crack Initiation and Propagation in a Two-Dimensional Triangular Lattice**, (Ph. D. Dissertation, University of California at Davis-Livermore, 1983).
[34]. E. Meiburg, Phys. Fluids 29, 3107(1986).

[35]. B. J. Alder and T. E. Wainwright, Phys. Rev. Letters 18, 988 (1967).
[36]. W. G. Hoover, B. Moran, R. M. More, and A. J. C. Ladd, Phys. Rev. A 24, 2109(1981).
[37]. M. Mareschal and E. Kestemont, J. Stat. Phys. 48, 1187(1987); M. Mareschal, M. M. Mansour, A. Puhl, and E. Kestemont, Phys. Rev. Letts. 61, 2550(1988).
[38]. E. N. Lorenz, J. Atmos. Sci. 20, 130 (1963).
[39]. G. Benettin, L. Galgani, and J. M. Strelcyn, Phys. Rev. A114, 2338 (1976); I. Shimada and T. Nagashima, Prog. Theor. Phys. 61, 1605 (1979).
[40]. W. G. Hoover and H. A. Posch, Phys. Lett. 113A, 82 (1985) and 123A, 227 (1987).
[41]. W. G. Hoover, H. A. Posch, and S. Bestiale, J. Chem. Phys. 87, 6665 (1987).
[42]. H. A. Posch and W. G. Hoover, Phys. Rev. A38, 473 (1988).
[43]. H. A. Posch and W. G. Hoover, Phys. Rev. A39, (to appear 1 February, 1989).
[44]. J. Salmon, Hadronic Journal 3, 1080(1980).
[45]. S. Nosé, Mol. Phys. 52, 255(1984) and 57, 187 (1986).
and J. Chem. Phys. 81, 511(1984).
[46]. W. G. Hoover, Phys. Rev. A31, 1695 (1985).
[47]. W. G. Hoover, Lecture Notes in Physics, Vol. 258, Molecular Dynamics (Springer-Verlag, Berlin, 1986).
[48]. D. J. Evans and B. L. Holian, J. Chem. Phys. 83, 4069(1985).
[49]. B. L. Holian, J. Chem. Phys. 84, 3138(1986).
[50]. W. G. Hoover, H. A. Posch, B. L. Holian, M. J. Gillan, M. Mareschal, and C. Massobrio, Mol. Sim. 1, 79(1987).
[51]. B. L. Holian, W. G. Hoover, and H. A. Posch, Phys. Rev. Letts. 59, 10(1987). B. L. Holian, G. Ciccotti, W. G.

Hoover, H. A. Posch, and B. Moran, Phys. Rev. A (to appear, 1989).
[52]. W. G. Hoover, Phys. Rev. A37, 252(1987).
[53]. J. Ford, "Directions in Classical Chaos", in Directions in Chaos, Vol. 1, p. 1, H. Bai-Lin, ed. (World Scientific, Singapore, 1988).
[54]. B. Mandelbrot, The Fractal Geometry of Nature (W. H. Freeman, San Francisco, 1982).
[55]. B. Moran, W. G. Hoover, and S. Bestiale, J. Stat. Phys. 48, 709 (1987); W. G. Hoover, B. Moran, C. G. Hoover, and W. J. Evans, Physics Letters A, 133, 114(1988).
[56]. A. J. C. Ladd and W. G. Hoover, J. Stat. Phys. 38, 973(1985). G. P. Morriss, Phys. Rev. A (to appear, 1989).
[57]. G. P. Morriss, J. Stat. Phys. 44, 107(1986); G. P. Morris, Phys. Lett. 113A, 269 (1985); G. P. Morriss, Phys. Rev. A 37, 2118 (1988).
[58]. L. A. Pars, A Treatise on Analytical Dynamics (Oxbow Press, Woodbridge, Ct., 1979).
[59]. G. Casati, I. Guarneri, and D. L. Shepelyansky, IEEE J. Quant. Electronics 24, 1420(1988).
[60]. R. W. Hasse, Rep. Prog. Phys. 41, 1027(1978).
[61]. A. O. Caldeira and A. J. Leggett, Physica 121A, 587(1983).
[62]. H. Dekker, Phys. Rev. A 16, 2126(1977).

FIGURE CAPTIONS

Figure 1. Harmonic-oscillator trajectory *via* the classic fourth-order Runge-Kutta method, using six steps per period to illustrate the approximate nature of the calculation. The exact trajectory is a periodic ellipse.

Figure 2. 16-spring anharmonic oscillator chain studied by Fermi, Pasta, Ulam, Tuck, and Menzel at Los Alamos. The typical starting condition was the lowest-frequency "mode" shown in the Figure, with quadratic or cubic forces added to the Hooke's-Law linear forces.

Figure 3. Trajectory time exposures for three-dimensional hard spheres in the solid(left) and fluid(right) phases, from Reference [11]. Pictures such as these showed that purely-repulsive forces are sufficient to cause freezing.

Figure 4. Cover of the August 1959 Journal of Applied Physics. The boundary particles obey irreversible viscoelastic equations of motion.

Figure 5. Three-phase temperature-density phase diagrams for the Lennard-Jones pair potential, from molecular dynamics and Monte-Carlo simulations(solid), and for Argon, from experiment(dashed).

Figure 6. DNA, as seen using a scanning tunneling microscope, as described in Reference [23].

Figure 7. Boundary conditions for simple shear or heat flow. The two sets of four shaded "Fluid-wall" particles, at the top and bottom of the Figure, are enclosed by pairs of horizontal reflecting walls. These fluid-wall particles interact across these walls with the twelve Newtonian

Particles shown in the central region. The fluid-wall particles obey time-reversible thermostatted equations of motion.

Figure 8. Four types of boundary conditions for simulating fluid or solid deformation. The motions are driven by (i) external fluid-wall particles, (ii) homogeneous periodic deformation, (iii) inhomogeneous external fields, and (iiii) moving corrugated boundaries.

Figure 9. Fragmentation simulation showing over 14,000 two-dimensional Lennard-Jones atoms in free expansion from a hot compressed state.

Figure 10. Fracture simulation showing an arrested crack in a crystal with a tapered boundary under tension. The imposed tensile stress caused the crack to proceed past the stopping point, indicated by arrows, predicted by static fracture mechanics.

Figure 11. Hard-sphere simulation of flow past a splitter plate. Each arrow represents the averaged velocity of about 50 hard spheres. The beginnings of a "vortex street" can be seen.

Figure 12. Time- and space-averaged fluid flow velocity vectors in a two-dimensional simulation of compressible Rayleigh-Bénard heat flow in a vertical gravitational field. The two vortices found with molecular dynamics match the predictions of continuum mechanics, as described in Reference [37].

Figure 13. Schematic time-development of a phase-space hypersphere into a short-time hyperellipsoid, and a longer-time Smale horseshoe.

Figure 14. Bouncing of a mass point on an infinitely-massive elastic ball of unit radius. The maximum height of the bouncing point is 1.25. Plotting the same trajectory on a semilogarithmic scale (at right) shows the characteristic Lyapunov instability responsible for macroscopic irreversibility.

Figure 15. Typical Lyapunov-exponent spectra for two- and three-dimensional fluids and solids. The phase-space stretching rates (positive Lyapunov exponents) and compression rates (negative Lyapunov exponents) are shown as symmetric Smale pairs. This equilibrium symmetry is broken in the nonequilibrium states discussed in Section VI.

Figure 16. Computer-generated snake on a computer-generated fractal background.

Figure 17. Sierpinski sponge generated from a cube by repeatedly removing 7/27 of the remaining mass. The mass remaining after N such removals is $(20/27)^N$. As N diverges the resulting object becomes a zero-volume fractal object with a fractal dimensionality of 2.727.

Figure 18. Galton Board trajectory Poincaré section showing the history of successive colllisions for a single mass point moving through the board. The Board geometry and a unit cell are shown to the right. Each point in the phase-space section on the left indicates a collision. The abscissa angle α measures the location of the collision relative to the field direction. 0 and π correspond respectively to collisions at the bottom and the top of a scatterer. The ordinate measures the (sine of the)

angle β, relative to the normal, of the moving particle's velocity after each collision. Glancing collisions correspond to angles of $\pi/2$ or $-\pi/2$. A head-on collision corresponds to $\beta = 0$. The "hole" corresponds to an exceptional and interesting isolated set of quasiperiodic Kolmogoroff-Arnold-Moser collisions which are not connected to the main chaotic phase space.

Figure 19. Two Galton Board ensemble Poincaré sections showing the time-development of two ensembles, each with 2500 mass points moving independently through Galton Boards of the same type, and with the same field as shown in Figure 18. The development of the ensembles after 1, 2, 3, 5, and 10 collisions is shown.

Figure 20. Three steps linking mechanics, dynamics, and irreversible thermodynamics.

Figure 21. Mass distribution in a steady-state solution of the quantum Galton Board using the nonequilibrium form of Schrœdinger's Equation described in Section VI. The 41x41 grid is centered on a scatterer which excludes 613 of the 1681 sites from occupancy. The time-dependent Gaussian modification of Schrœdinger's equation is then solved for the 1068 nonvanishing values of the real and imaginary wave-function. In the flow illustrated here, the average flow velocity is about half the thermal velocity, which is in turn about ten times less than the maximum thermal velocity allowed by the finite-difference grid. The quantum-momentum wavelength corresponding to this solution is about 40% of the cell width. The left view is a snapshot of the mass distribution. The right view is a time average over two wave-traversal times.

Figure 22. Momentum distribution in the steady-state solution of the quantum Galton Board, as shown in Figure 21, using the nonequilibrium Schrœdinger equation described in Section VI. The left view is a snapshot of the momentum distribution. The right view is a time average. The current flow is primarily negative so that the plotted values lie below the zero associated with the 613-site elastic scatterer.

Figure 23. Energy distribution in a steady-state solution of the quantum Galton Board, as shown in Figure 21, using the nonequilibrium Schrœdinger equation described in Section VI. The left view is a snapshot of the energy distribution. The right view is a time average. Note the similarity of this time average to the mass average shown in Figure 21.

Figure 24. Boltzmann, Gauss, Hamilton, Lyapunov, Newton, and Schrœdinger.

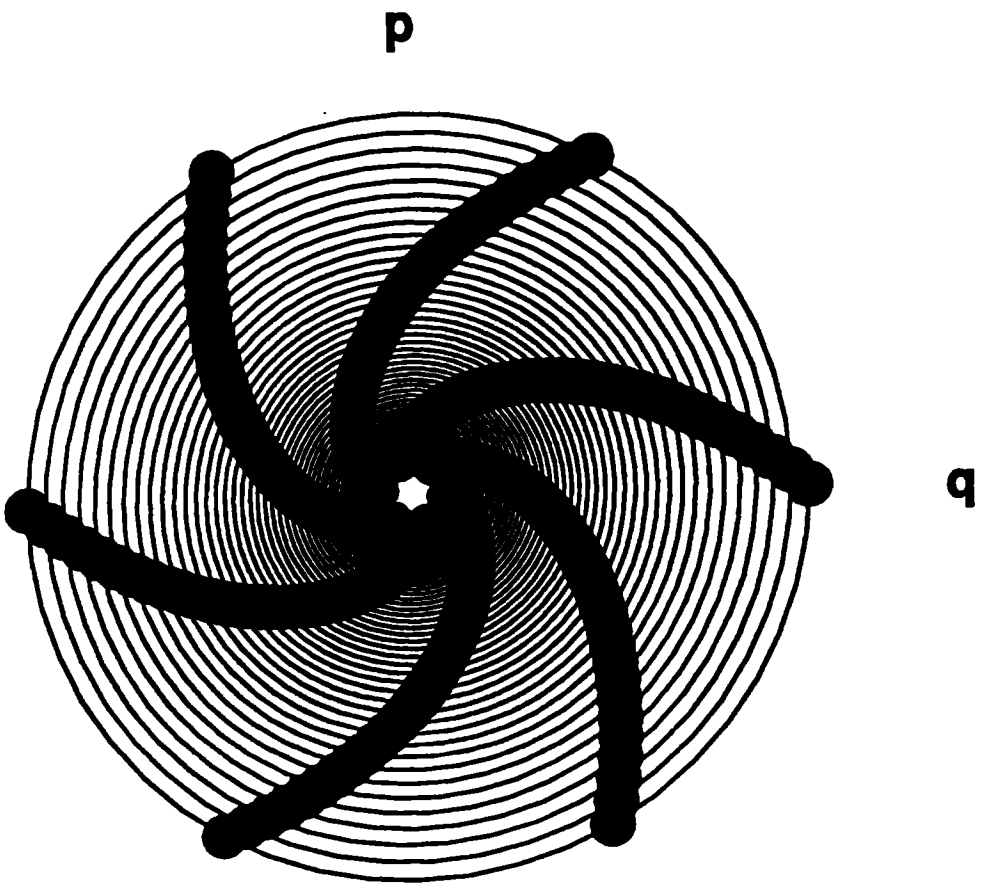

FIGURE 1

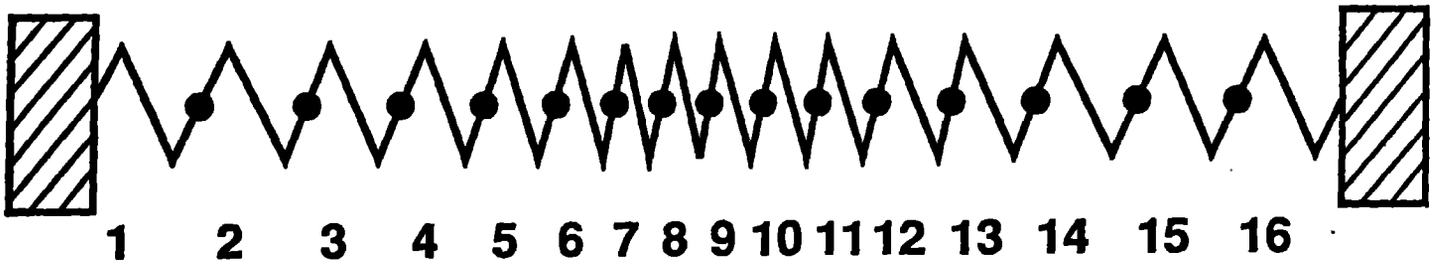
1 2 3 4 5 6 7 8 9 10 11 12 13 14 15 16

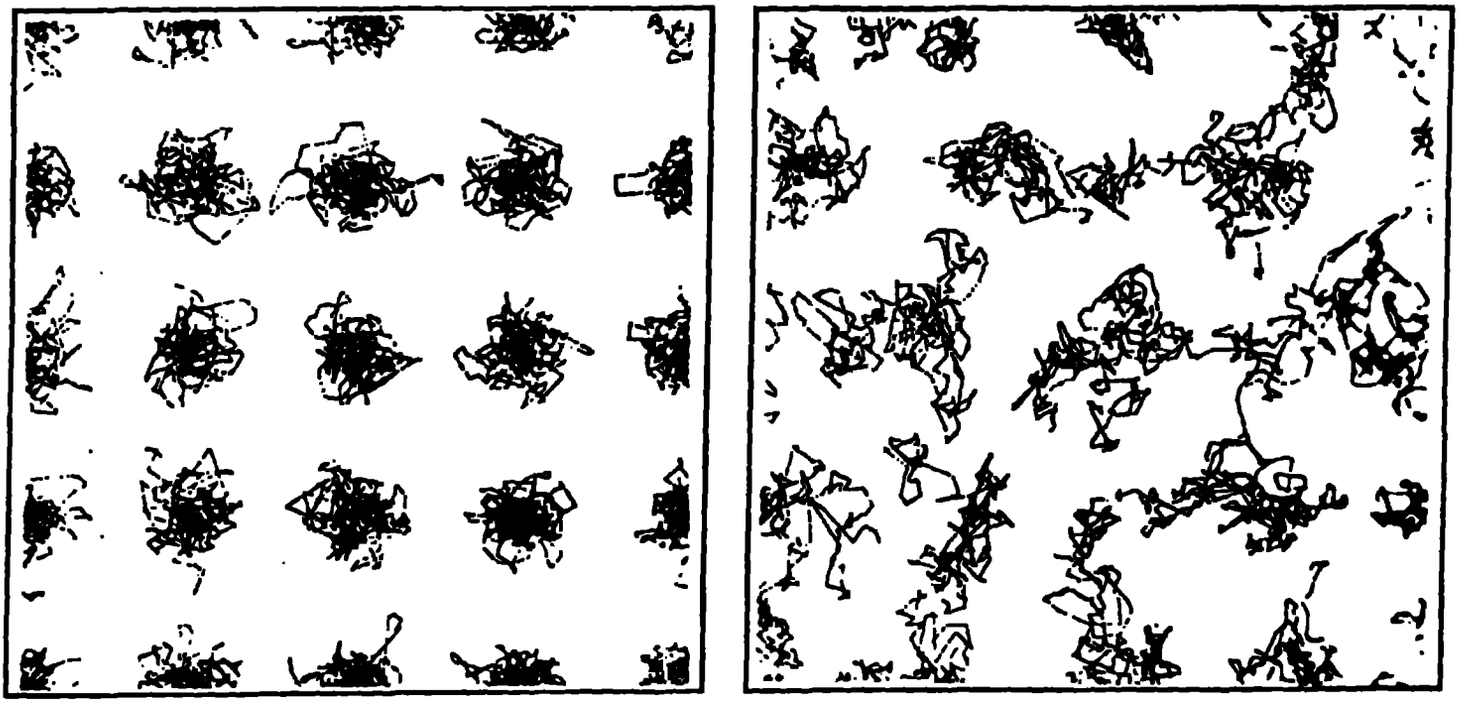

Figure 3

JOURNAL
OF
APPLIED PHYSICS

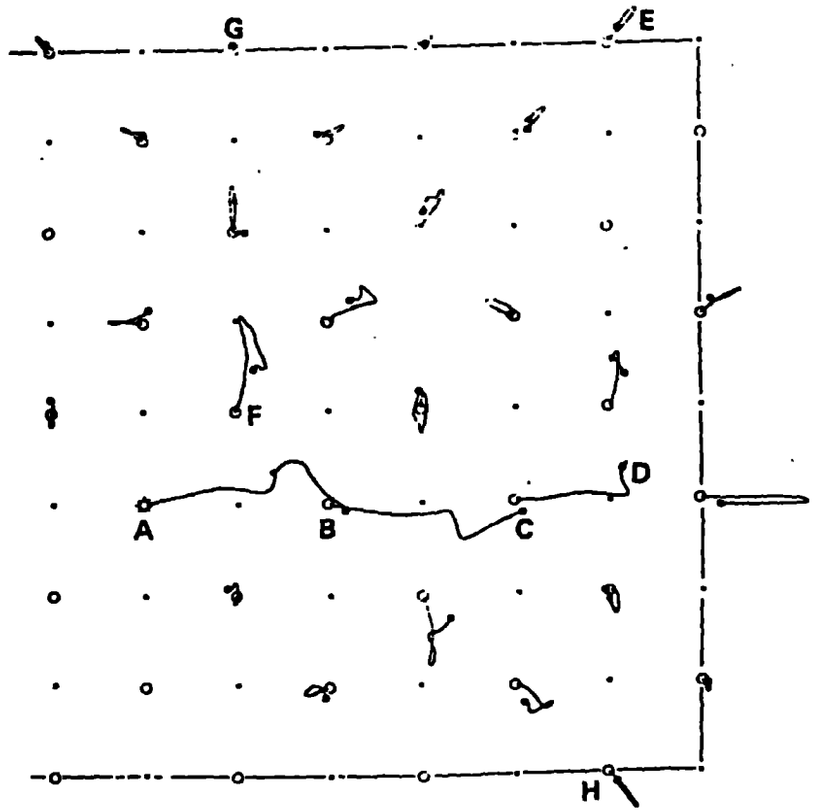

40 eV in (100) plane
15° off [100] direction
Pot. #2

Atoms in plane
- Time 0
- Time 99

Atoms in planes above and below
- Time 0

Figure 4

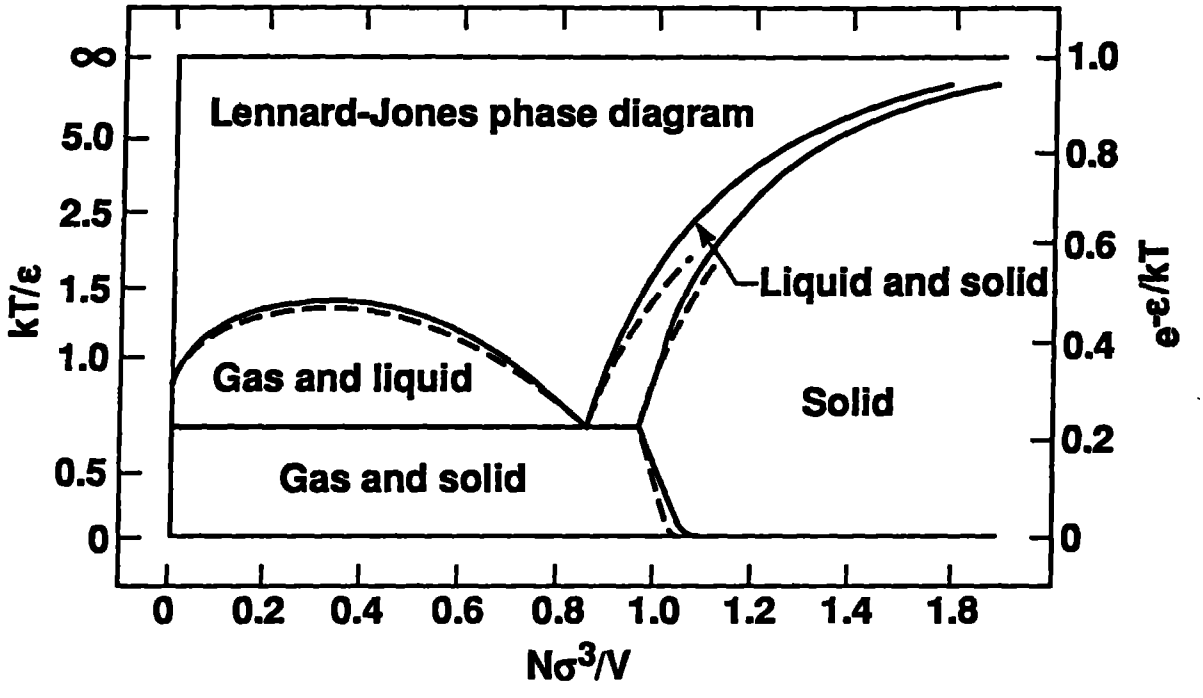

TF-S5-U-2838-Fig5A

Figure 5

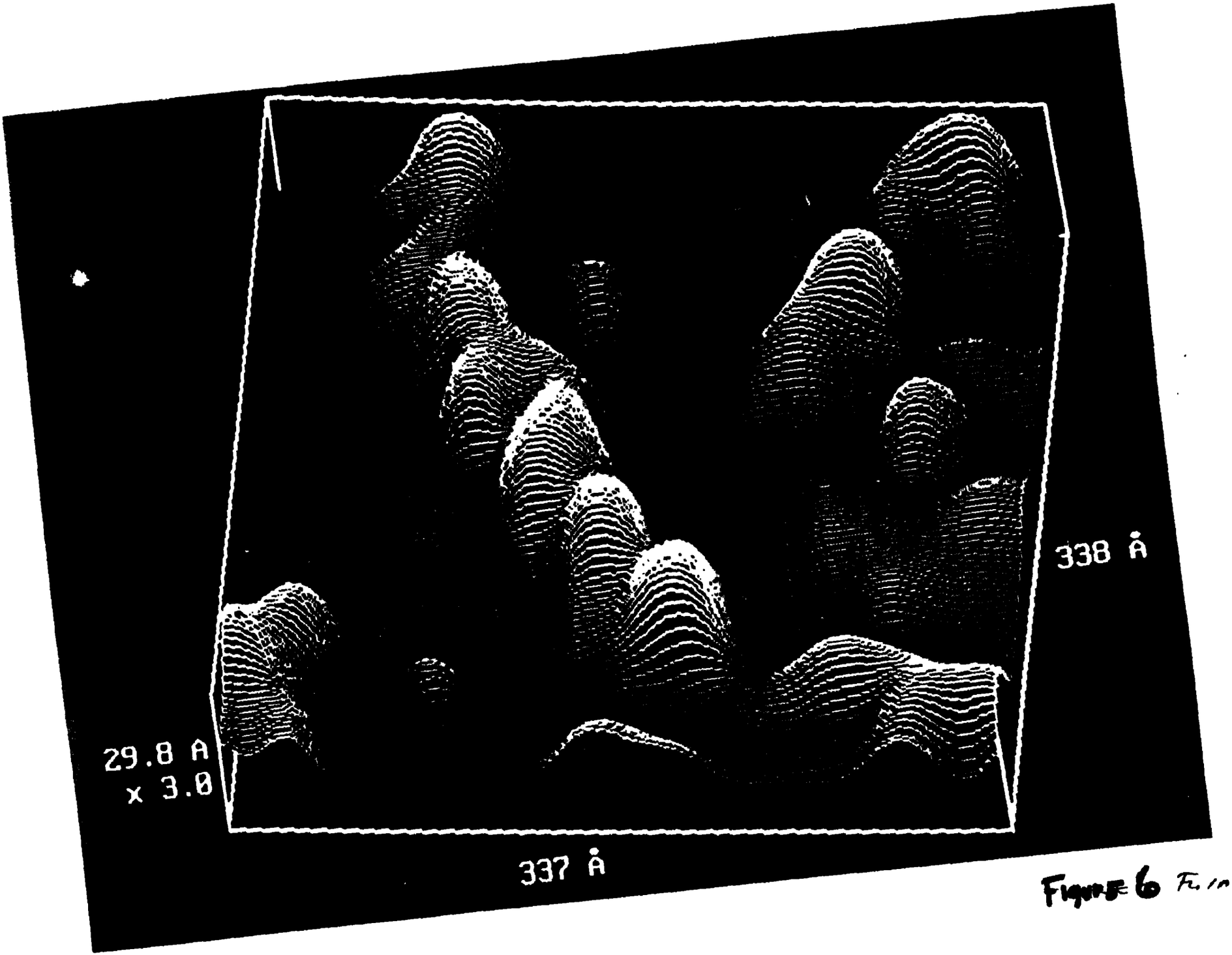

Figure 6 Film

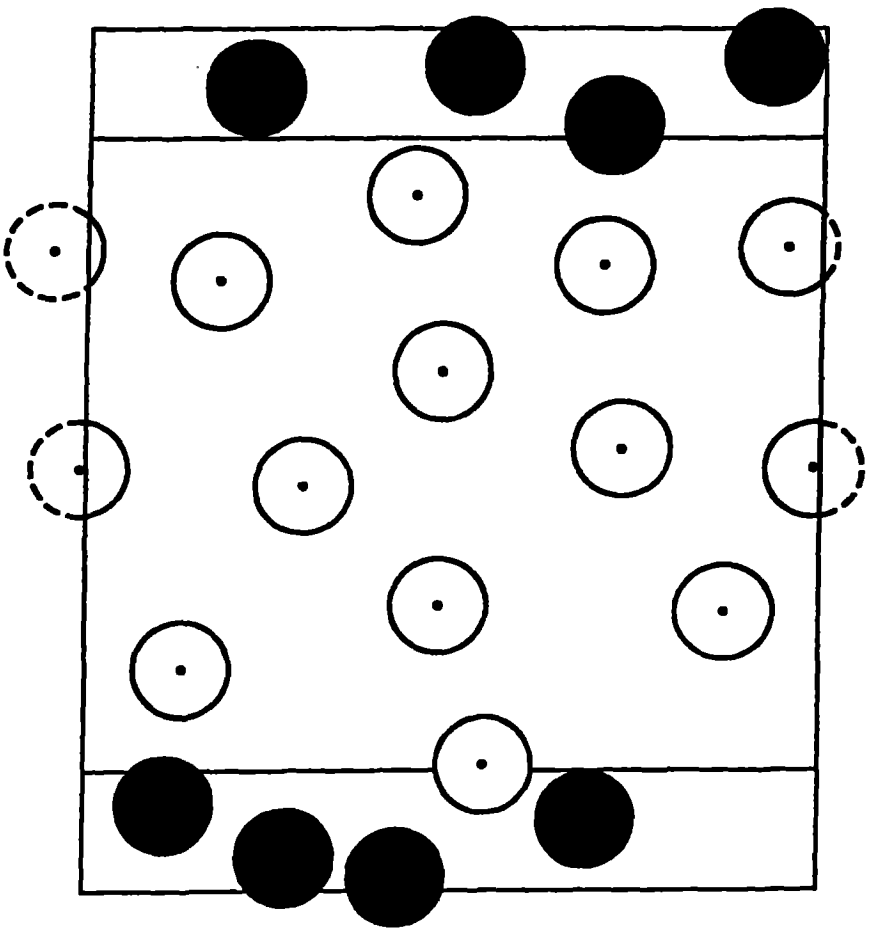

CW-S23-U-2838-F7

Figure 7

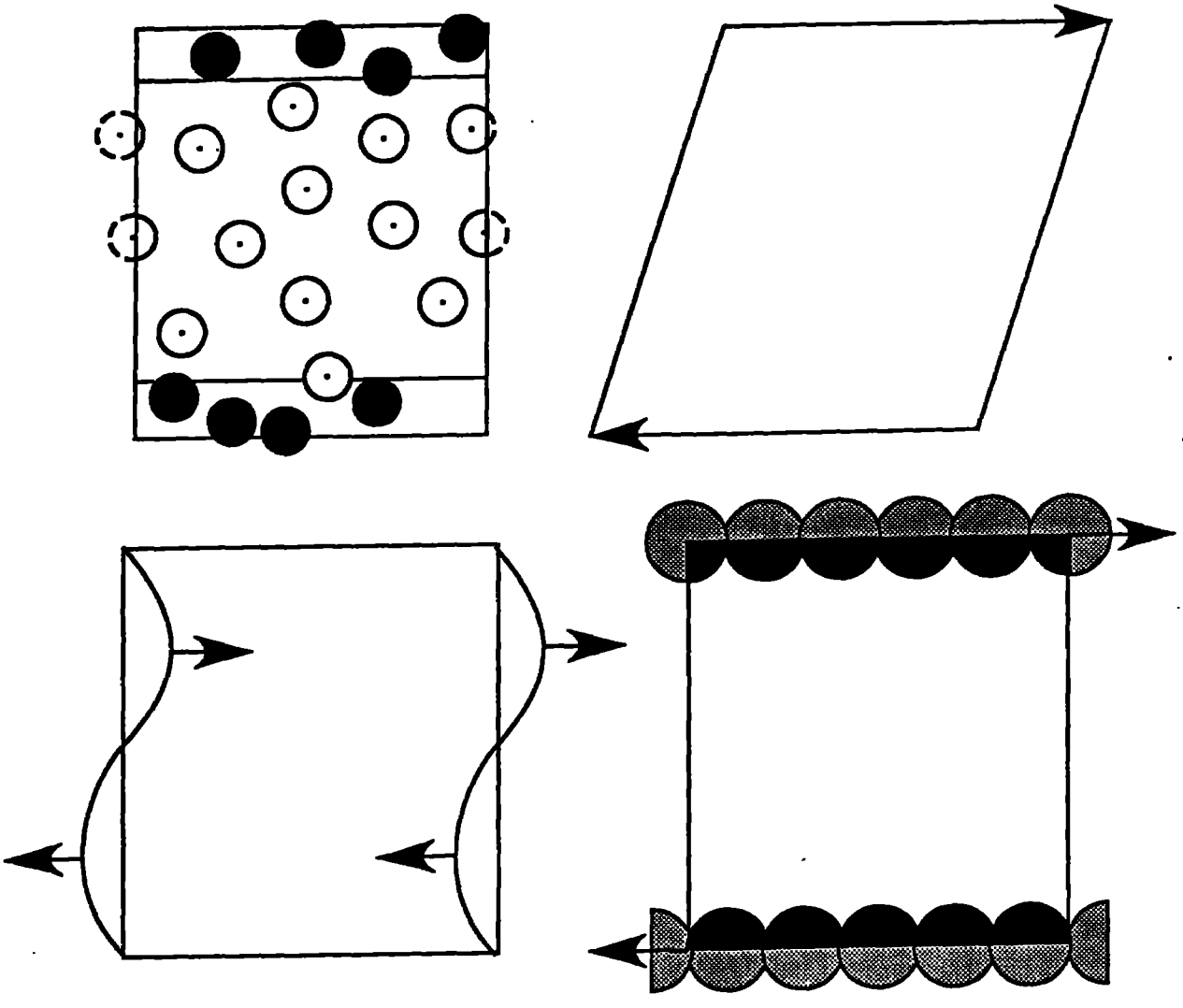

LAD-S23-U-2838-F8

Figure 8

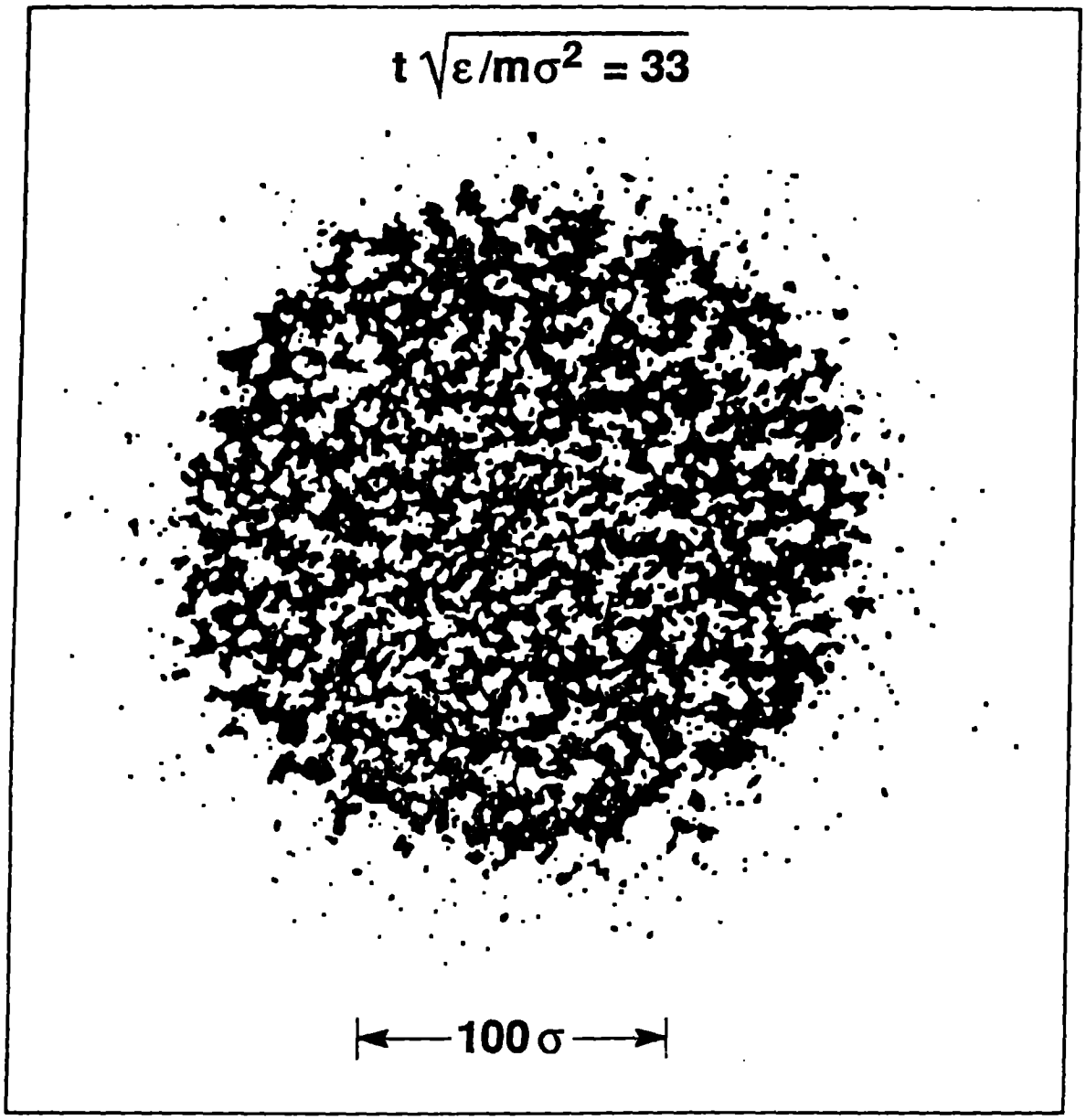

Figure 9

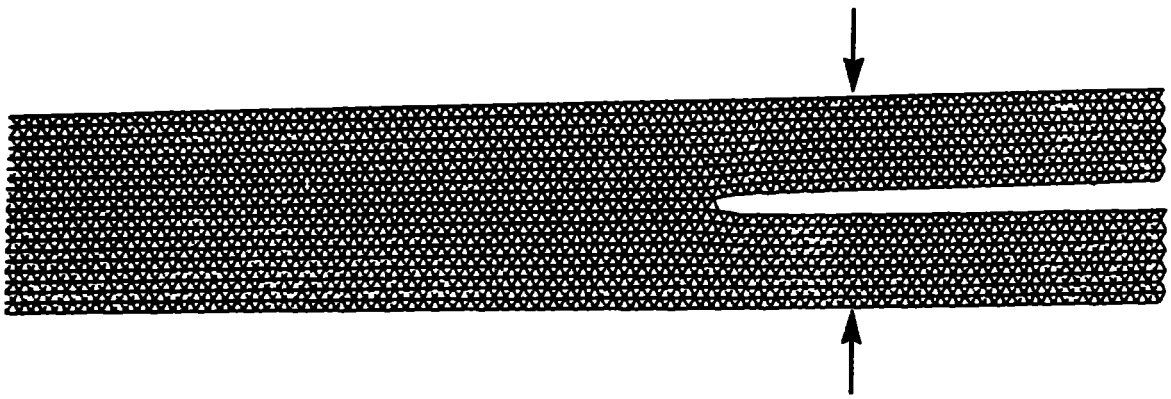

Figure 10

WO# 2858
F. 10

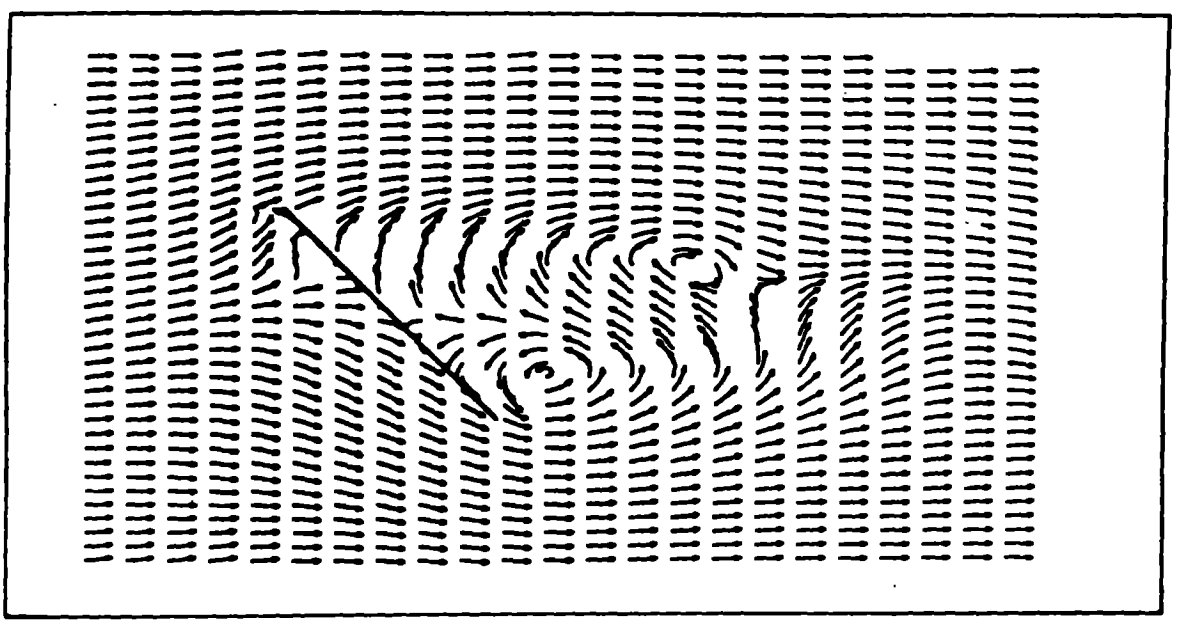

WO# 2858
F. 11

Figure 11

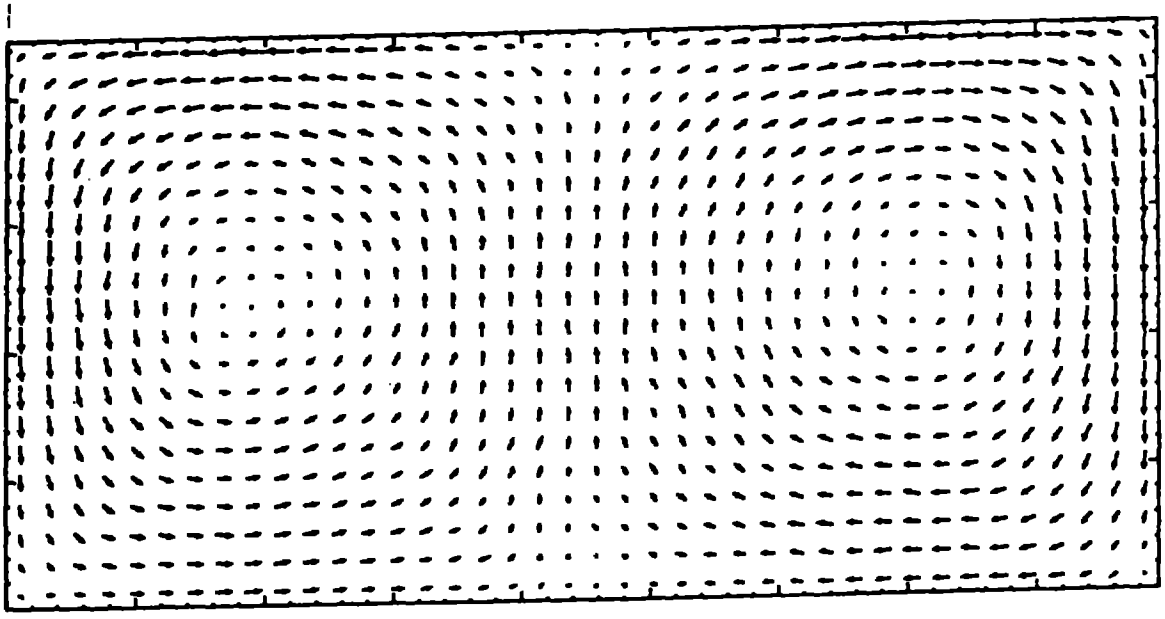

Figure 12

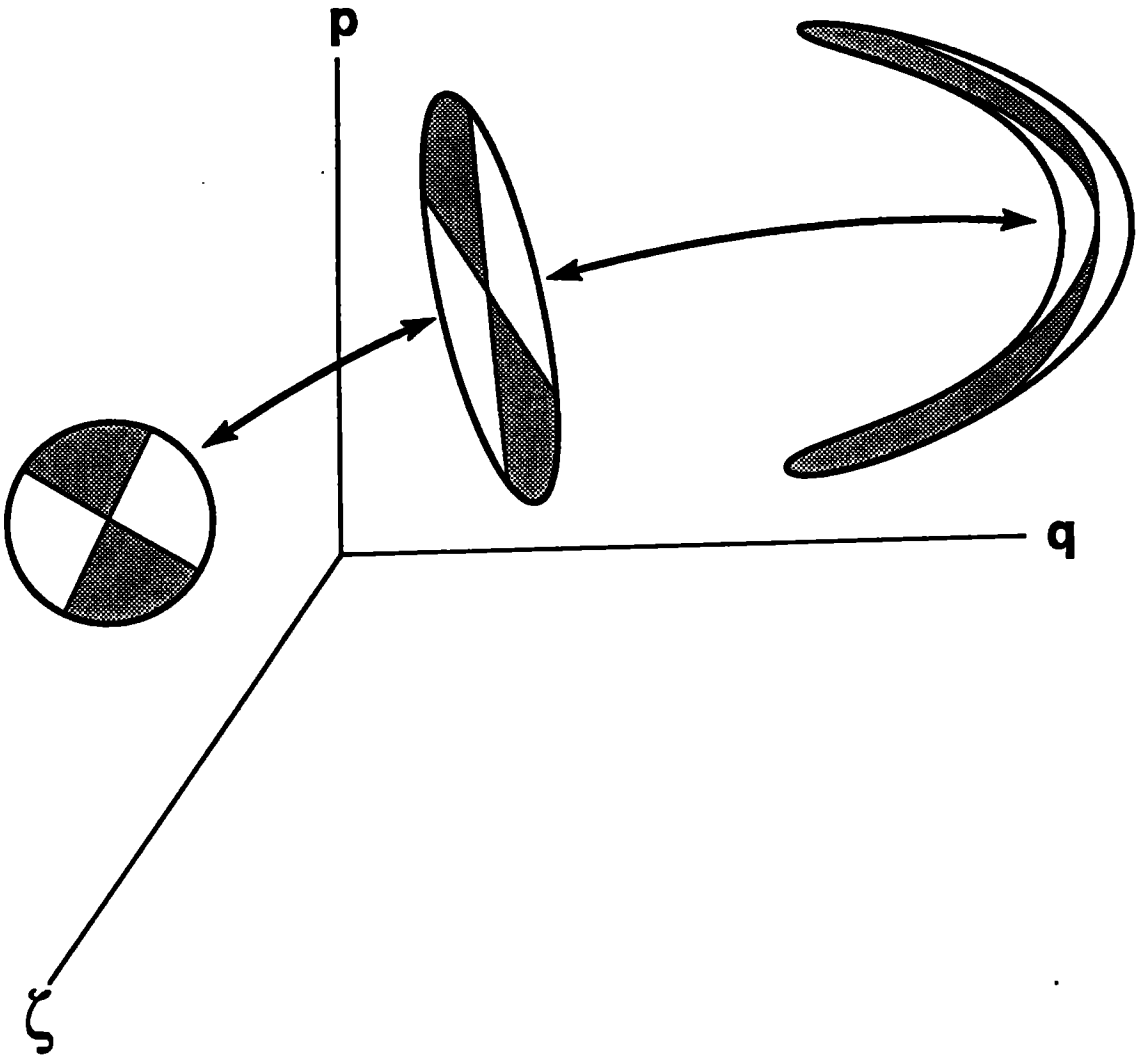

SKL-S25-U-2838-13

Figure 13

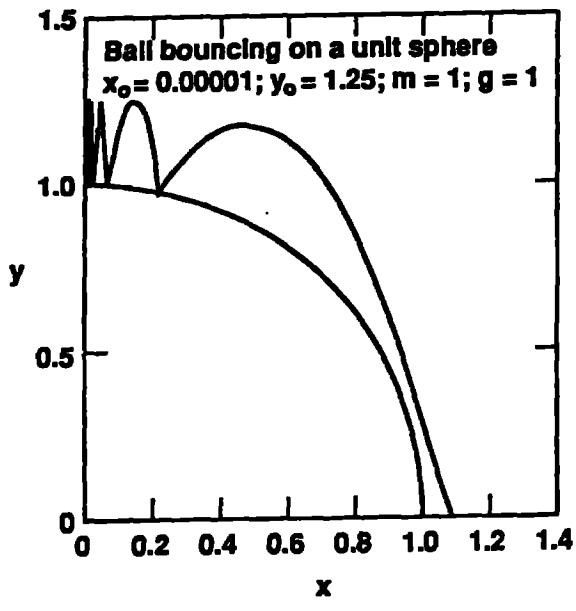
Ball bouncing on a unit sphere
x_o= 0.00001; y_o = 1.25; m = 1; g = 1
1.5
1.0
0.5
0
y
0
0.2
0.4
0.6
0.8
1.0
1.2
1.4
x

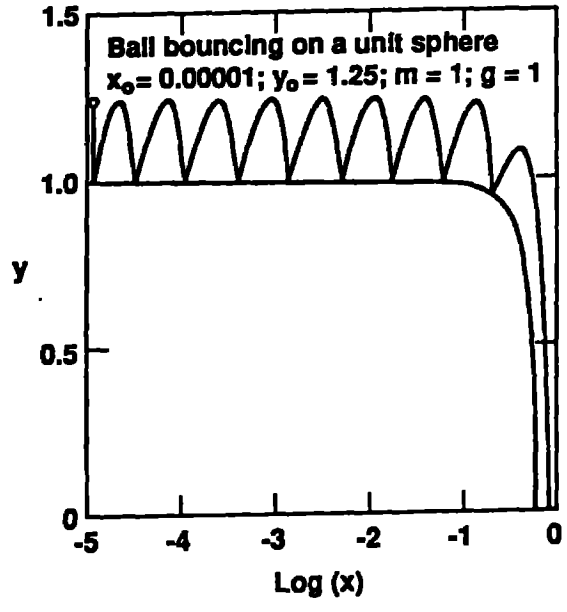
Ball bouncing on a unit sphere
x_o= 0.00001; y_o = 1.25; m = 1; g = 1
1.5
1.0
0.5
0
y
-5
-4
-3
-2
-1
0
Log (x)

Figure 14

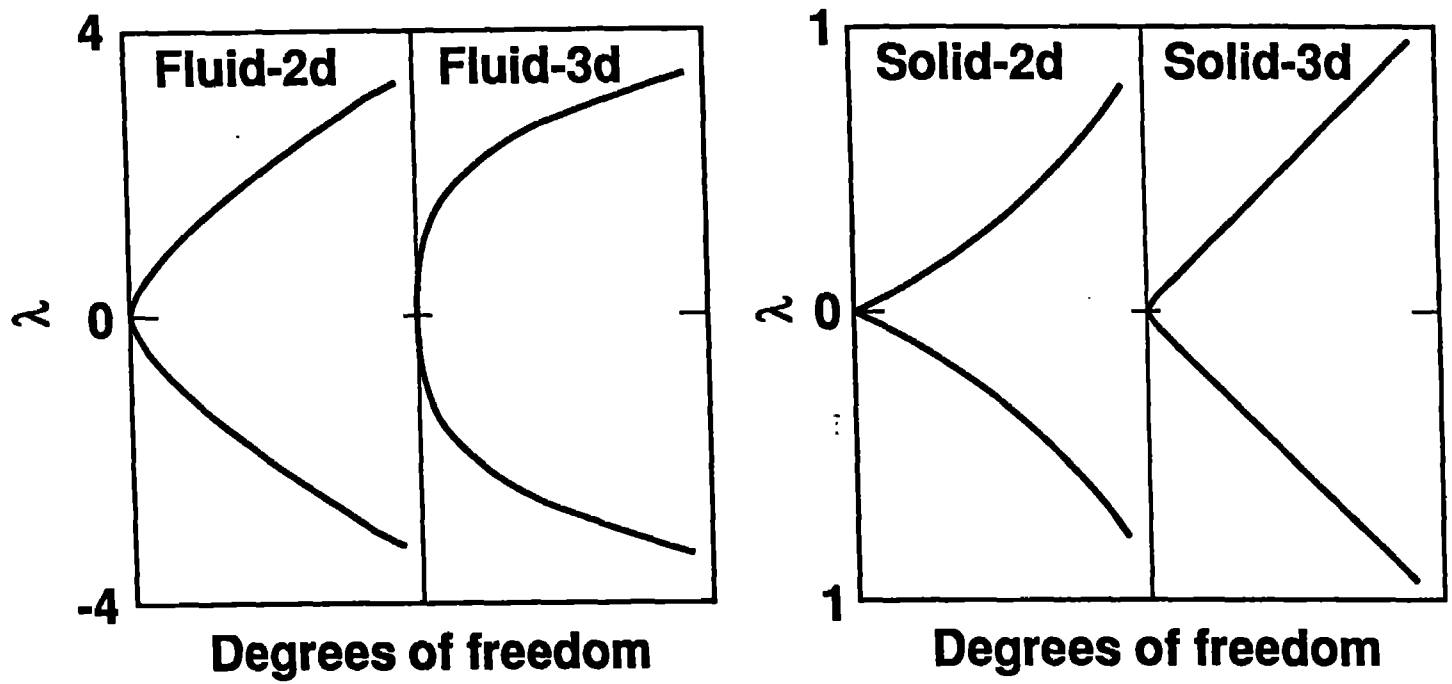

Figure 15

PT-S18-U-2639-15A

Figure 16

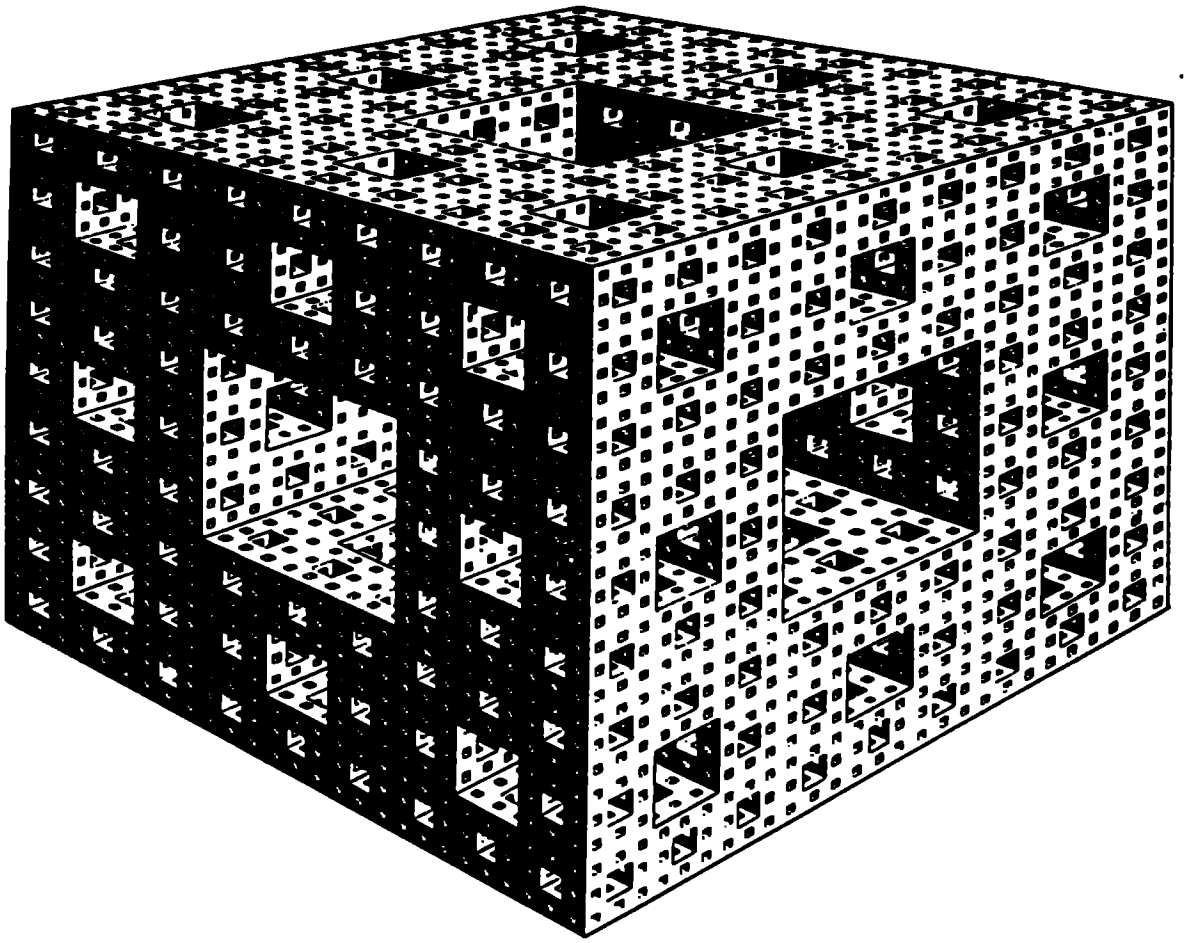

wo# 2838
F. 17

Figure 17

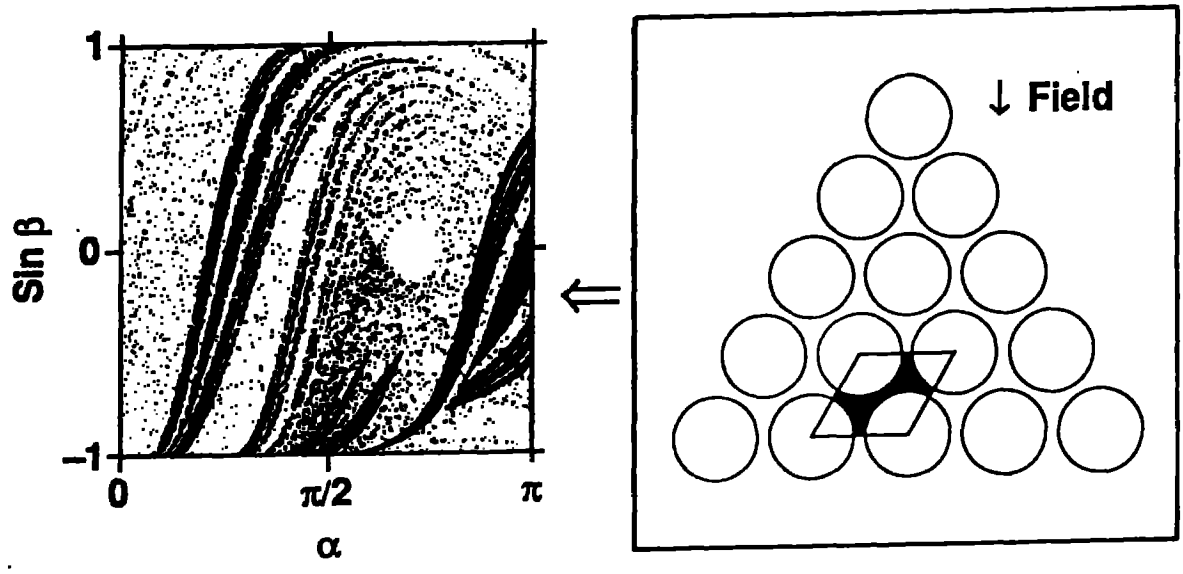

Figure 18

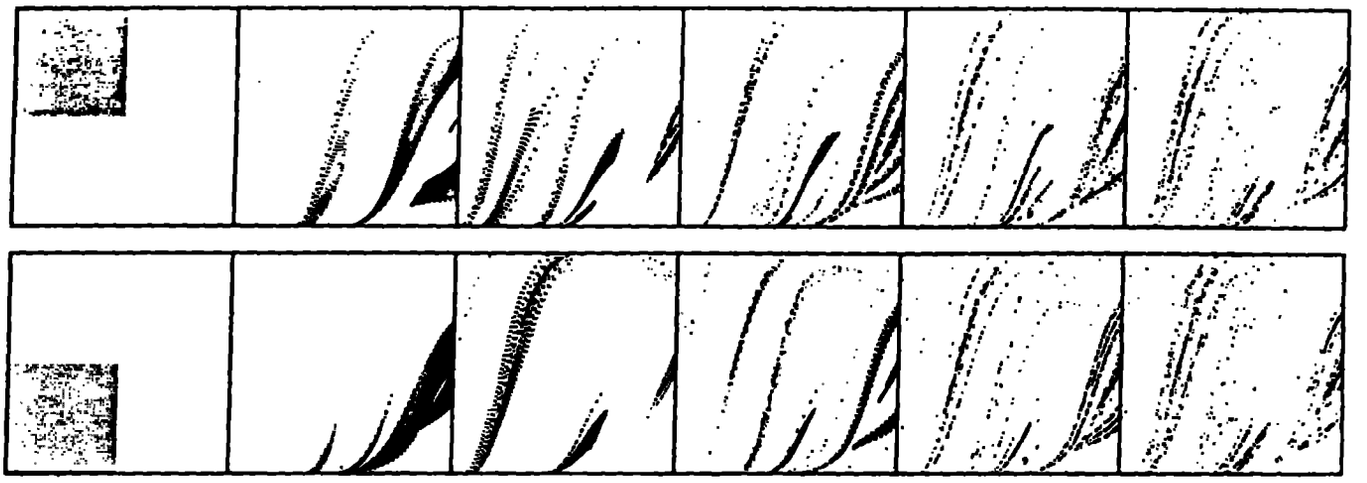

Figure 19

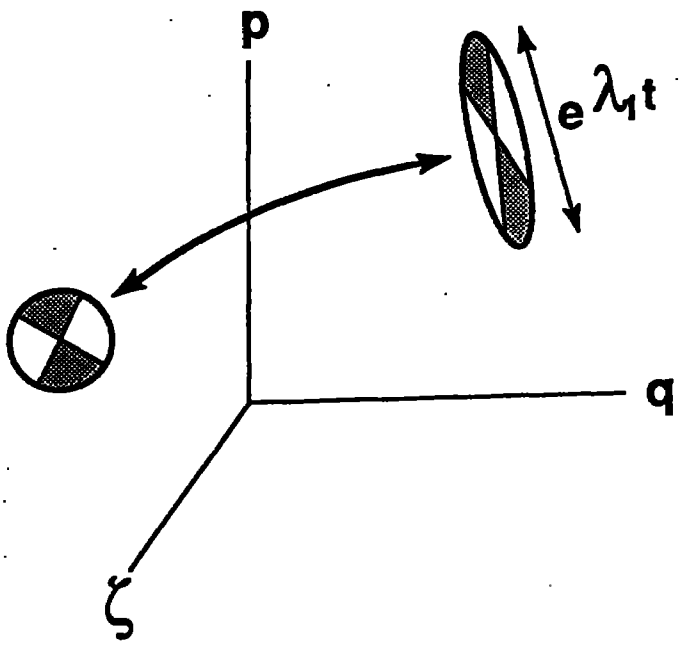

I and II:

$$d\ln f/dt + d\ln \otimes/dt \equiv 0;$$
$$\Sigma\zeta + \Sigma\lambda \equiv 0;$$

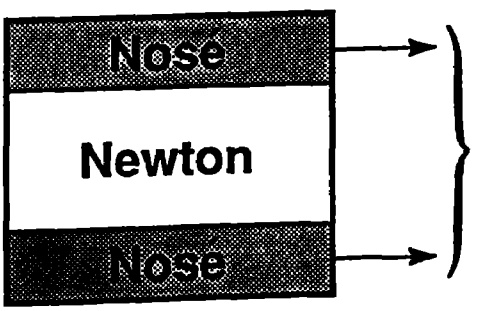

III:

$$\Sigma\lambda < 0 \Rightarrow \Sigma\zeta > 0.$$

$$\Sigma\left[\frac{dQ/dt}{T}\right] = \Sigma\zeta = \frac{d(S/k)}{dt}.$$

Figure 20

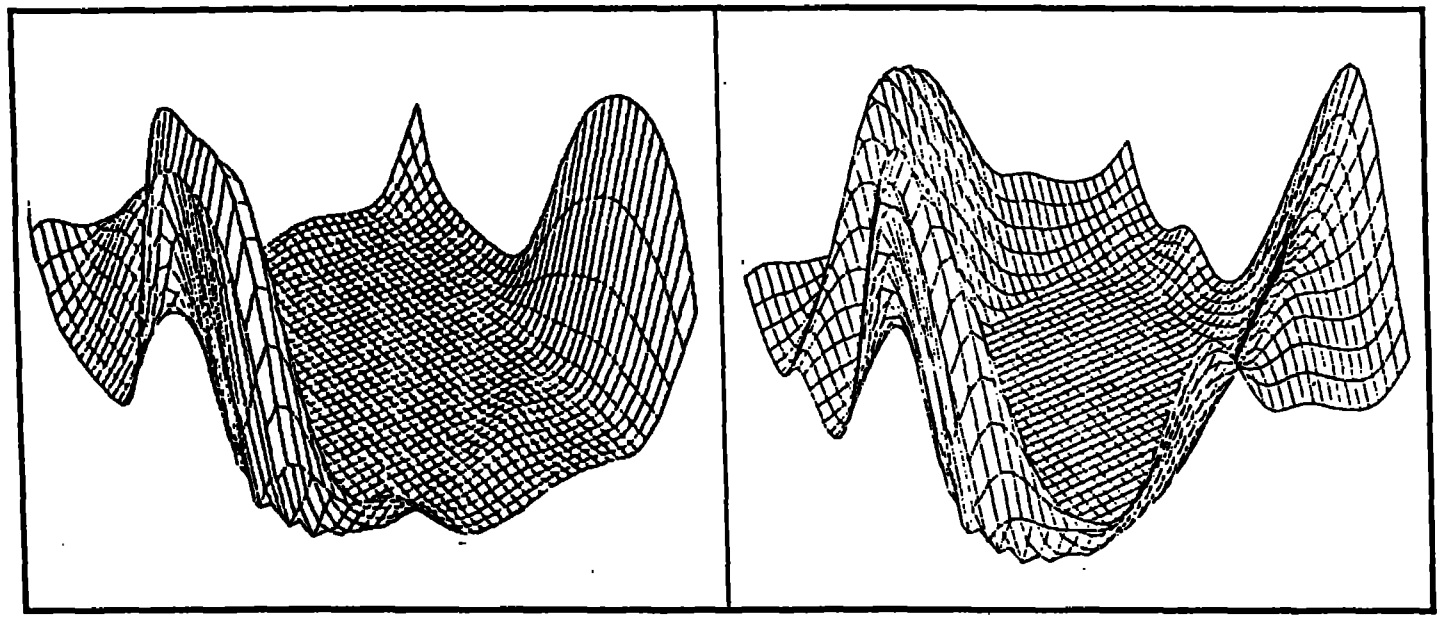

Mass

Figure 21

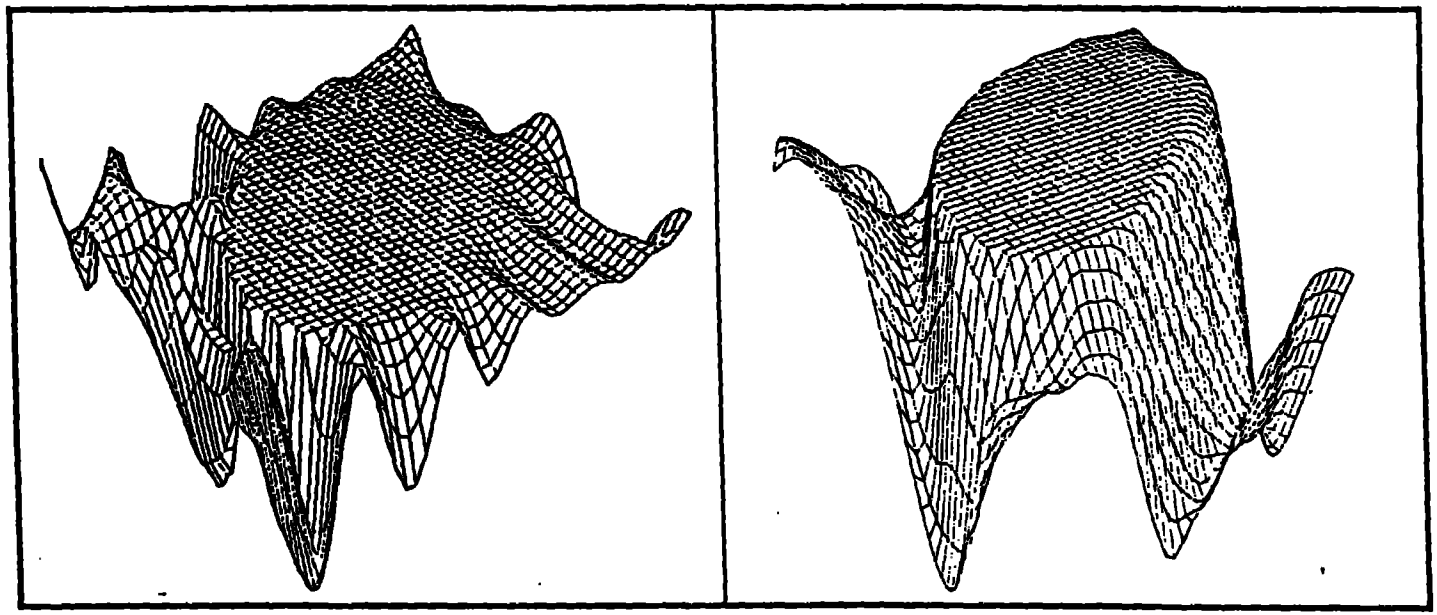

Momentum

Figure 22


REPUBLIKOSTERREICH
S 3
1844 1906
75.Todestag des Physikers
BOLTZMANN
C.F.GAUSS * 1777 † 1855
DEUTSCHE BUNDESPOST
10
1843 eire 1943
2½
ROWAN HAMILTON
ВЕЛИКИЙ РУССКИЙ МАТЕМАТИК
А.М.ЛЯПУНОВ
1857
1957
40
ПОЧТА СССР
REPUBLIQUE FRANÇAISE
18F
NEWTON
1642-1727
ERWIN SCHRÖDINGER 1887-1961
S 5
REPUBLIKÖSTERREICH

Figure 24

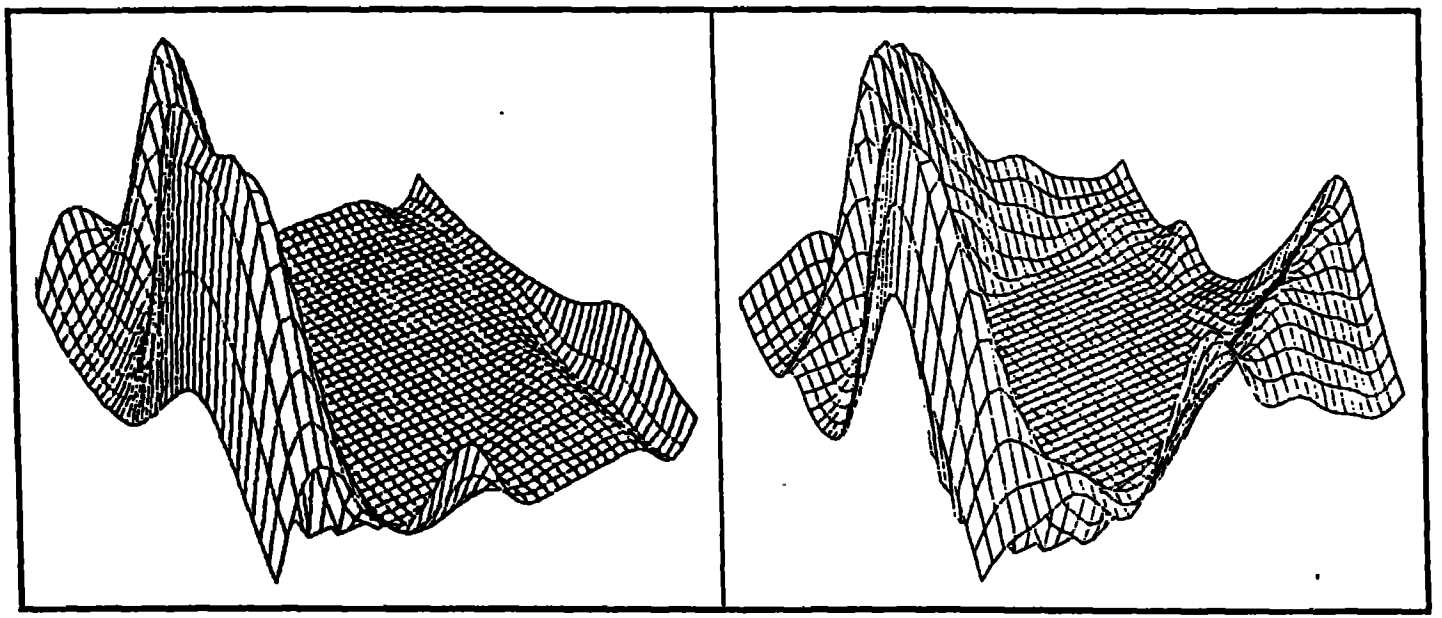

Energy

figure 23